

Reference

NBS  
Publi-  
cations

NAT'L INST. OF STAND & TECH. R.I.C.



A11101 731264

A11105 891024

NBSIR 81-2209 (FDA)

# Relationship Between Morphology and Mechanical Properties of Ultra High Molecular Weight Polyethylene

---

G. B. McKenna, Ph.D.  
Principal Investigator

F. A. Khoury, Ph.D.  
Project Leader

J. M. Crissman, Ph.D.  
Project Leader

First Annual Report for the Period  
December 9, 1980 - September 30, 1980  
Task 80-01, NBS-BMD Interagency Agreement

April 1981



QC

100

.U56

81-2209

1981

DEPARTMENT OF COMMERCE

NATIONAL BUREAU OF STANDARDS



DEC 7 1981

NBS 81-2209

Q-10

U.S.

NO. 81-2209

1981

NBSIR 81-2209 (FDA)

**RELATIONSHIP BETWEEN MORPHOLOGY  
AND MECHANICAL PROPERTIES OF  
ULTRA HIGH MOLECULAR WEIGHT  
POLYETHYLENE**

---

G. B. McKenna, Ph.D.  
Principal Investigator

F. A. Khoury, Ph.D.  
Project Leader

J. M. Crissman, Ph.D.  
Project Leader

First Annual Report for the Period  
December 9, 1980 - September 30, 1980

Task 80-01, NBS-BMD Interagency Agreement

April 1981

**U.S. DEPARTMENT OF COMMERCE, Malcolm Baldrige, *Secretary***  
**NATIONAL BUREAU OF STANDARDS, Ernest Ambler, *Director***



## Abstract

Aspects of the morphology of the constituent particles of the raw ultra high molecular weight polyethylene (UHMWPE) used in this study have been examined using scanning electron microscopy. In addition differential scanning calorimetry has been used to determine the melting point ( $\sim 413\text{K}$ ) and the crystallinity (78%) of the raw polymer. Protocols have been established for the preparation of compression molded sheets of UHMWPE having crystallinities of 50% and 60%. A memory of the particulate nature of the raw polymer is retained in the sheets. There was a considerable variation in the sizes of the birefringent structures in the sheets, the majority were extremely small and barely visible under the polarizing microscope, the larger among these structures appeared to be axialitic or incipiently spherulitic. The following aspects of the mechanical behavior of the molded sheets have been examined: Stress-strain behavior at constant rate of clamp separation, creep and single step stress relaxation in uniaxial extension, and failure under both static and sinusoidal loading conditions. The relaxation modulus of the lower density material (quenched) was found to be smaller by a factor of two than that of the higher density material (slow cooled). The short time creep of the quenched UHMWPE was significantly greater than that of the slow cooled polymer; however, the limiting creep strain prior to failure was nearly the same for both materials. Low cycle fatigue data obtained on the slow cooled UHMWPE suggests that it may be possible to characterize the failure behavior of this polymer using a cumulative damage rule. The lifetime of the UHMWPE under zero-tension sinusoidal loading is 6-7 times longer than the lifetime in static (creep) tests in agreement with the cumulative damage rule. Over the range of frequencies tested (0.0002-0.01 Hz) limited data show no trend of lifetime dependence on test frequency. Results of the failure testing indicate that the static lifetime of UHMWPE may be a lower

bound on the zero-tension fatigue lifetime. A study of the fine structure changes resulting from uniaxial deformation under constant rate of clamp separation has also been started. In addition an apparatus has been built for the study of the equal biaxial deformation of UHMWPE sheets in air as well as in the presence of stress-cracking agents. Experiments, using this equipment are currently under way.

## Table of Contents

Abstract .....	i
Table of Contents .....	iii
1. Introduction .....	1
2. Background .....	2
3. Experimental Methods and Results .....	5
3.1 Raw Polymer Characterization .....	5
(a) Morphology .....	5
(b) Melting Behavior .....	7
(c) Crystallinity .....	8
3.2 Specimen Preparation and Characterization .....	8
(a) Molding Conditions and Specimen Densities and Morphology .....	8
3.3 Mechanical Properties .....	14
(a) Stress-Strain Behavior at Constant Rate of Clamp Separation .....	14
(b) Uniaxial Creep .....	19
(c) Stress Relaxation .....	20
(d) Failure Studies .....	23
(e) Equal-Biaxial Deformations Under Inflation and Environmental Stress Cracking .....	27
(f) Miscellaneous .....	29
4. Summary .....	30
5. Work Plan for FY 1981 .....	34
Appendix A .....	36
References .....	37
Figures .....	40



## 1. Introduction

Ultra high molecular weight polyethylene, hereafter referred to as UHMWPE, is used in a variety of orthopedic implant devices because of its chemical inertness and mechanical durability. In some applications, for example the acetabular component of the total hip replacement, UHMWPE has proven successful, and under proper clinical conditions may perform effectively for 15 to 20 years. However in other applications, such as knee and ankle prostheses, UHMWPE components have had only limited success. The increased use of such devices in more youthful patients will require material performance beyond 20 years. In addition to the materials aspect of overall performance there is clearly a need for better design particularly for knee and ankle prostheses. At the present time there is little evidence of new and better materials appearing in the marketplace. It remains to be determined whether UHMWPE has been exploited to the limits of its capabilities. Insights into what these limits may be requires detailed knowledge and understanding of the time dependent mechanical behavior of the polymer and the influence of factors such as molecular weight, crystallinity and morphology on its mechanical behavior.

The work being carried out under task 80-01, NBS-BMD Interagency Agreement addresses principally the relationship between morphology and the time dependent mechanical properties of UHMWPE. It is our view that the accomplishment of the primary objectives outlined below will be of significance both to the FDA Bureau of Medical Devices and to the medical device industry. These objectives are:

- (1) To investigate and determine the influence of polymer morphology on the time dependent mechanical properties of UHMWPE, and thereby identify the fine structure parameters which significantly affect long term performance.

- (2) To obtain data on creep and stress relaxation (both in compression and tension) behavior, as well as time dependent failure. Such data will be useful as a basis for the design and evaluation of current and future devices made from UHMWPE.
- (3) To devise measurement techniques relevant to the development of standard test methods for characterizing the time dependent mechanical properties of implants based on UHMWPE.

## 2. Background

One obvious factor which limits the expected lifetime of hip, knee, or other joint prostheses is the durability of the UHMWPE component. In clinical use, failure of the polymer component is not a result of wear alone, but may occur through creep [1]\*, fatigue associated with wear [1,2], or even fracture [3,4]. The length of time between device implantation and clinical failure will depend upon the time dependent mechanical response of the material in the clinical loading situation.

It is known that the time dependent mechanical response of semi-crystalline polymers is highly affected by such structure or morphology related features as degree of crystallinity, orientation, and spherulite size and texture [5,6]. For example, in work performed in our laboratory it was found that the stress relaxation behavior of UHMWPE, not unlike that of lower molecular weight polyethylenes, is highly sensitive to annealing [7]. Through annealing of an as received sample the percent crystallinity (as determined from density measurements) increased from 56% to 67%; at the same time the one second torsion modulus increased from 280 MPa to 350 MPa. More importantly, the rate of stress decay was significantly lower in the annealed material.

---

\* Numbers in brackets refer to references located at the back of this report.

In the case of UHMWPE there are additional factors which must be considered when studying the dependence of mechanical properties on morphology. One such factor is the presence of a "grain memory" [7,8]. By grain memory we mean that the finished part has a fine texture which reflects, in part, that of the nascent polymer. It is possible that the grain memory affects performance. Another factor affecting performance is the processing, that is, the temperature and pressure history used in manufacture. A thermal history which brings about an improvement in one property may actually result in the diminution of another. For example, increasing the degree of crystallinity of low molecular weight polyethylene increases the modulus, yet at the same time it decreases the resistance to brittle fracture and stress cracking. Also, because of the very high molecular weight of UHMWPE the melt viscosity is very high. The proper fusion of the polymer grains therefore becomes an important aspect of processing. In a study of the impact fatigue of various commercial grades of UHMWPE, Bhatega, Rieke, and Andrews [9] reported that the poor performance of one material was associated with incomplete fusion of the polymer powder. Finally, in a study of wear surfaces [10], cracking has been observed to occur at intergrain boundaries.

It is apparent that the time dependent mechanical behavior of UHMWPE depends upon morphology and/or processing in a variety of ways. In order to better understand this dependence we are studying the creep, stress relaxation, and dynamic and static fatigue behavior of specimens of compression molded material having significantly different degrees of crystallinity. At the same time the morphology of these specimens is being examined as a function of both the preparation conditions and deformation history. One objective of this work is to determine the range of material property variability which

can be introduced by changes in crystallinity.

A word is in order concerning the types of tests commonly used to evaluate the mechanical properties of polymers, for example those recommended by ASTM. Such tests tend to measure short term behavior, and the results obtained may not predict long term performance. Based on recent work performed in our laboratory the following examples serve to illustrate this point. In low molecular weight polyethylenes the failure mode in uniaxial creep depends upon the magnitude of the applied stress. At high stresses (short times to failure) the material undergoes large deformations involving necking, cold-drawing, and eventual fracture. On the other hand at low stresses (long times to fail) failure occurs by cracking and fracture at small elongations [11]. In another study of the fatigue behavior of low molecular weight polyethylenes it was found that the failure mode depended upon the test frequency, changing from a ductile mode at low frequency to a brittle-like mode at higher frequency [12]. The behavior of UHMWPE under conditions comparable to those just described remains to be determined. In the case of the low molecular weight polyethylenes it was also found that the lifetime was shorter under static loading than it was under cyclic loading (for an equivalent peak load). If this behavior is also true of the UHMWPE, then the determination of fatigue life under a given load history is simplified since the static measurements would represent a lower bound on the fatigue life. Static testing is significantly easier to perform and is less time consuming than is dynamic testing.

Finally, we recognize that wear is an important aspect of performance of devices made from UHMWPE. Wear is a phenomenon which is influenced by a number of factors including the time dependent mechanical properties of the material, as well as the chemical and load environments [13]. Wear in prosthetic components made from UHMWPE appears to be accompanied by both large scale deformation and cracking of the surface region [14,15]. In our view, the wear phenomenon cannot be understood until morphology-mechanical property relationships

are better established.

### 3. Experimental Methods and Results

#### 3.1 Raw Polymer Characterization

Unless otherwise stated the compression molded samples prepared for the studies described in this report were all made from the same batch of commercial implant grade ultrahigh molecular weight polyethylene. For purposes of identification this batch will henceforth be identified as UH-A. The raw polymer as received was in the form of a powder (see below), and to our knowledge contains no additives such as antioxidant or stabilizers. The intrinsic viscosity (limiting viscosity number) of UH-A is approximately 25\*, which, based on the manufacturer's method of estimating molecular weight from dilute solution viscosity measurements, corresponds to a molecular weight of  $\sim 4 \times 10^6$ .

Three aspects of the raw polymer were examined namely, its morphological characteristics, its melting behavior, and its crystallinity. These features are described below:

##### (a) Morphology.

The polymer, as received, is in its as polymerized (i.e. nascent) state and consists of fine particles. As indicated in Section 2, earlier studies [7,8] of the morphology of both molded and machined prosthesis components made from UHMWPE have shown that a memory of the particulate (or grain-like) nature of the raw polymer is retained even though the polymer was heated well above its melting point in the manufacturing process. This feature,

\* The determination of intrinsic viscosity from dilute solution viscosity measurements is subject to a number of problems and uncertainties which have been discussed in detail by Wagner and Dillon [16]. The definition of "ultra high" molecular weight is under consideration by two ASTM committees, Committee F-4 on Implant Devices and Committee D-20 on Plastics. In the case of F-4 the criterion for use of the term 'ultra high' is that the intrinsic viscosity should be  $\approx 15$  or higher, whereas in the case of D-20 it should be  $\approx 21$  or greater. The UH-A meets both criteria.

which may be attributed to the extremely high viscosity of the molten polymer, was readily observed in thin ( $\sim 50 \mu\text{m}$ ) cross-sections examined under a light microscope at low magnifications using phase contrast optics. Under those conditions, the boundaries between the compacted nascent particles were seen throughout the cross-sections. This observation emphasizes the importance of characterizing the structure of UHMWPE products, not only to determine their crystallinity, axialitic or spherulitic texture, and lamellar fine structure, but also to monitor those aspects of their morphology which are directly related to, and a consequence of, the particulate nature of the raw polymer and its high melt viscosity. Knowledge of the morphology of the raw polymer is therefore a necessary aspect of the present study since the nature of the shapes, sizes, and fine textures, of nascent polyethylene particles vary depending on the polymerization conditions [17,18].

Scanning electron micrographs showing nascent particles of UH-A are shown in Figs. 1, 2a, and 3a. Portions of the particles in Figs. 2a, 3a, are shown at higher magnifications in Figs. 2b, 2c, and Figs 3b, 3c respectively. Prior to examination the particles had been sputtered in an Argon atmosphere with an Au:Pd (40%/60%) alloy in order to prevent charging upon exposure to the electron beam.

Numerous particles can be seen in Figs. 1a,1b which illustrate their irregular shapes and varying sizes. Their sizes generally range from  $\sim 80 \mu\text{m}$  to  $\sim 300 \mu\text{m}$ . It is evident from these figures as well as Figs. 2a, 3a that the surfaces of the particles are highly convoluted. At low magnification (e.g. Fig. 1) the external appearance of the individual particles resembles that of compact bunches of grapes. Examination at higher magnification

reveals that whereas portions of the surface of the particles are relatively smooth, others exhibit a highly porous appearance, as can be seen in Figs. 2a, 2b, and Figs. 3a, 3b. At even higher magnifications (e.g. Figs 2c, 3c) the gaps or voids in the porous regions can be seen to be bridged by thin fibrils which are 50 nm-100 nm in diameter. The various origins of fibrils in nascent polyolefins have been reviewed by Marchessault et. al. [17]. It appears that in the case of the UH-A particles, the bridging fibrils result from the deformation of the polymer during polymerization as a consequence of the progressive expansion of the particles caused by the continued generation of fresh polymer at the surface of underlying encapsulated catalyst.

(b) Melting Behavior,

Differential scanning calorimetry (DSC) was used to examine the melting behavior of the UH-A raw polymer. Unless otherwise specified the heating rate used during the melting scan was 10°C/min. At this heating rate the temperature correction for machine lag was determined to be 0.47K. For this particular UHMWPE (i.e. UH-A) the temperature corresponding to the maximum in the melting peak was 418.3K (145°C). Upon subsequent cooling and remelting the temperature corresponding to the peak maximum in the melting peak dropped to the 408K-411K (135°C-138°C) range depending upon how rapidly the specimen was cooled following the first melting. It is typical of crystalline polymers such as polyethylene that their melting points vary according to their previous thermal and mechanical histories, and are lower than the equilibrium melting point, i.e. the melting point of an ideal extended chain crystal of the polymer (~419K, 146°C) [19]. The observed melting point of the raw polymer was, however, unusually high. This suggested the manifestation of 'superheating' at the heating rate of 10°C/min.

In order to determine whether this was the case a series of experiments was carried out in which specimens of fresh raw polymer were heated to various temperatures at which partial melting occurred. The specimens were then held for two hours at the chosen "dwell" temperature in each case after which heating was continued. The dwell temperature corresponding to which no further melting was observed upon subsequent heating was found to be between 413K and 414K (140°C-141°C), thus indicating that 'superheating' occurred at a heating rate of 10K/min and that the true melting point of the raw polymer is at least 5K lower than 418.3K.

(c) Crystallinity.

The crystallinity of the raw UH-A polymer was determined by DSC to be 78% using the procedure outlined in Appendix A. As will be seen in the following section this crystallinity is much higher than that in compression molded sheets made from UH-A which were slowly cooled from the molten state.

### 3.2 Specimen Preparation and Characterization

(a) Molding conditions and specimen densities and morphology.

Because of its very high molecular weight and consequent very high melt viscosity the type of UHMWPE polymer used in this study cannot be processed by conventional techniques such as injection molding or standard extrusion. The sheets of polymer used in this study were successfully prepared by compression molding. Initially, sheets were molded according to the procedure recommended by the polymer manufacturer. This method consists of a ten step process in which the polymer is heated to temperatures as high as 478 to 493K (205 to 220°C). However, the sheets produced in this manner showed considerable yellowing around the edges, indicative of degradation. As a result, a good deal of effort was devoted to the design of a vacuum mold and the development of molding

procedures by which specimens suitable for the mechanical testing could be prepared in a reproducible manner. After experimenting with different molding temperatures and pressures the following standard molding procedure was chosen in order to produce circular flat sheets approximately 15 cm in diameter and 0.1 cm thick.

- (1) The vacuum mold is filled with a predetermined amount of UHMWPE powder and placed in the press. The heat is then turned on, with only light contact pressure applied on the mold.
- (2) When the platens reach 408K (135<sup>o</sup>C) a pressure of 2.4 MPa (350 PSI) is applied on the mold for a short period of time and then released. The mold chamber containing the polymer is then subjected to vacuum.
- (3) The platens and mold are heated slowly to 473K (200<sup>o</sup>C) and held at that temperature for ten minutes.
- (4) A pressure of 8.25 MPa (1240 PSI) is applied to the mold and the heat turned off.
- (5) The press is then allowed to cool to room temperature before removing the mold. (Between 200<sup>o</sup> and 100<sup>o</sup>C the rate of cooling in the press was approximately 1<sup>o</sup>C/min.)

Specimens prepared in this manner had densities in the range 0.934-0.936 g/cm<sup>3</sup>. These densities, which were determined with a density gradient column at 293.3K, correspond to weight % crystallinities,  $\chi$ , of 58%-60% (see Appendix A).

The bulk properties of conventional low molecular weight polyethylenes are determined primarily by the crystallization conditions which govern the

crystallinity and the morphology of molded specimens. Although higher dwell temperatures above the melting point, and longer dwell times at these temperatures, tend to lead to a relative diminution of nucleation density (nuclei/unit volume) during subsequent crystallization at low or moderate undercoolings, the effect of melting conditions on the crystallinity of samples subjected to the same crystallization histories is negligible or secondary in the absence of any imposed extensional flow. A complication does arise however in the case of the UHMWPE. As pointed out in Sections 2 and 3.1a, previous studies have shown that a memory of the particulate nature of the raw polymer is retained in compression molded samples. Since one would expect that the mechanical properties of the UHMWPE will be influenced by the effectiveness of the compaction, fusion, and "adherence" of the raw polymer particles, the question which arises is "what is a suitable maximum temperature at which compression molding should be carried out?". This aspect was examined as part of the process which led to the choice of the set of molding conditions described above. Sheets of UHMWPE were molded using a maximum temperature which was varied from 463K to 503K with all other conditions held the same. The densities of the sheets were in the range 0.934-0.936 g/cm<sup>3</sup>. Furthermore creep and single step stress relaxation measurements were made on samples from sheets molded at up to 483K. Within experimental error the sheets molded at different temperatures exhibited similar mechanical behavior. We have chosen 473K as our molding temperature. It is sufficiently high to permit proper flow of the material under pressure. At the same time there was no visual evidence of discoloration due to thermal degradation. This choice of molding temperature must be considered as somewhat arbitrary. It is, however, close to the low end of the molding temperature range recommended by the polymer manufacturer. It should be noted that as part of the background work leading to the choice of molding conditions, raw polymer samples were subjected

in a D.S.C. apparatus, to thermal treatments simulating the molding and crystallization procedures described above, i.e., the molding temperature prior to cooling was varied in the range 463K-503K. The melting behavior of the samples was found to be independent of the molding temperature used in that range.

Cross-sections approximately 50 $\mu$ m thick were cut at right angles to the plane of sheets made from the UH-A UHMWPE which had been molded at various temperatures in the range 463K-503K and which had subsequently been cooled slowly to room temperature as described above (as pointed out earlier the crystallinities of the sheets were 58%-60%). The cross-sections were examined under a light microscope using phase contrast optics. They were also examined between crossed polarizer and analyzer in a polarizing microscope.

Phase contrast micrographs of cross-sections microtomed from sheets molded at 463K, 473K and 503K are shown in Figs. 4(a,b,c). These figures clearly illustrate that a memory of the original coarse irregularly shaped particulate character of the raw polymer is retained in the molded sheets even in the case when molding was carried out at  $\sim$  90K above the melting point of the raw UH-A polymer. The pointed markers in Fig. 4 identify portions of a few interparticle boundaries.

Micrographs of portions of cross-sections of the same sheets molded at 463K, 473K, and 503K, are shown in Figs. 5, 6 and 7 respectively, all of which figures are at a higher magnification than in Fig. 4. Figs. 5a, 6a and 7a are phase contrast micrographs whereas Figs. 5b, 6b, and 7b represent, respectively, the same areas between crossed polarizer and analyzer. Figures 5b, 6b and 7b show that there are substantial variations in fine structure in each cross-section as evidenced by the differences in the size of the birefringent structural units from one region to another in each picture. In some regions the birefringent units are barely perceptible and

the corresponding areas exhibit a very fine grainy appearance under the polarizing microscope.

Although large well developed spherulites were not observed in these samples, rotation of the samples about the microscope axis while keeping the crossed polarizer and analyzer fixed indicated that some of the larger birefringent structural units were incipiently spherulitic or axialitic in character. Detailed studies of the effects of molecular weight and undercooling on the crystallization of polyethylene fractions from the melt have been reported by Hoffman et. al. [20] and Maxfield et. al [21]. A discussion of the morphology of polyethylene fractions is beyond the scope of this report. In the present context it suffices to indicate that the observed fine structures exhibited by the cross-sections in the polarizing microscope suggest that the absence of well developed spherulites is a consequence of a high nucleation density with the result that evolving spherulites impinged upon their nearest neighbors before attaining 'mature' spherically symmetrical shapes.\* The variations in the sizes of the birefringent structural units in the cross-sections shown in Figs. 5b, 6b, and 7b, are indicative of variations in nucleation density in each sample. Such variations may be attributed to localized variations in the compaction and flow of the raw polymer particles during the high temperature cycle of the compression molding process.

In addition to the types of slow cooled sheets described above, several sheets were prepared by rapidly quenching UHMWPE in the following manner. A sheet which had already been molded from UH-A polymer at 473K

---

\* Spherulites in polymers do not usually develop in a spherically symmetrical manner from the moment of inception. See reference [22] for a review and discussion of the nature of the early transitional stages of evolution of spherulites.

and slow cooled was placed between chromed metal photographic plates which were then placed in a press preheated to 473K. The plates were maintained at 473K for ten minutes under slight pressure and were then quickly removed from the press and immediately submerged into cold water. Sheets produced in this manner had a density of about 0.923 g/cm<sup>3</sup> which corresponds to a weight per cent crystallinity of 51% as compared to a value of 58%-60% for the slow cooled sheets. As was the case for the slow cooled samples, examination of cross-sections of quenched sheets under a light microscope revealed the retention of a memory of the particulate nature the original raw polymer even though those sheets had been subjected to an additional melting cycle. Furthermore, the quenched samples also exhibited under the polarizing microscope variations in the sizes of the birefringent structures in them.

In summary, protocols for preparing compression molded sheets of UHMWPE having weight per cent crystallinities of close to either 50% or 60% have been established. A maximum molding temperature of 473K has been selected. All the sheets were found to exhibit a memory of the particulate nature of the raw polymer and, on a finer scale, substantial variations were observed in the sizes of the birefringent structures in all the sheets.

### 3.3 Mechanical Properties

During the past year studies on mechanical properties were started in the following areas: stress-strain behavior at constant rate of clamp separation, creep and single step stress relaxation in uniaxial extension, and failure under both static and sinusoidal loading conditions. In addition preliminary work was done in equal biaxial deformation (under inflation) and on stress crack resistance. The emphasis thus far has been on the characterization of the mechanical behavior at room temperature of specimens slowly cooled from the melt. Some measurements have however been carried out on quenched sheets.

#### (a) Stress-Strain Behavior at Constant Rate of Clamp Separation

The specimens used for constant rate of clamp separation experiments were dumbbell shaped having a length in the gage section of 1.3 cm, a width of 0.32 cm, and a thickness of approximately 0.10 cm. In one set of experiments stress-strain curves were obtained for specimens slowly cooled from one of a series of melt temperatures ranging from 463K to 503K. It was found that the molding temperature had no significant influence on the stress-strain curve, in agreement with the findings discussed in Section 2. Curves representative of different rates of clamp separation at 296K are shown in Figure 8; the arrows indicate the point at which fracture occurred. These curves are typical of polyethylenes in general in that they are rate dependent. For the range of rates used in this study the breaking strength (stress at break) increased with increasing elongation rate whereas the elongation at break decreased. One interesting feature of the behavior of the UHMWPE, unlike that of lower molecular weight or some crosslinked polyethylenes, is that it does not neck but rather elongates in a uniform manner (on a macroscopic scale) right up to the point of fracture. Nusbaum

and Rose [23] claim to have observed necking in the fatigue testing of radiation sterilized UHMWPE. Whether the necking occurred as a result of the crosslinking or possibly was due to a significant reduction in molecular weight because of irradiation is unknown.

An indication of the effect of temperature on the stress-strain behavior of a slowly cooled specimen is illustrated in Fig. 8 in which a curve determined at 310K (37°C) is also shown. Comparison with the curve obtained at 296K at the same rate of clamp separation shows, not unexpectedly, that the elongation at break increased, and the breaking strength decreased with increasing temperature.

One aspect of the behavior of the slow cooled polymer sheets which is of interest in the context of implant performance is the appreciable recovery (contraction) exhibited by stretched samples when they are released at various strains below the breaking strain, as well as after they fail. For example the following observations were made in a series of experiments carried out at 310K. Two samples were stretched at a clamp separation rate of 0.04 in/min (corresponding to a strain rate of  $\approx 0.02$ /min). They both failed at a strain of 3.8. The broken samples were then kept at room temperature for twenty-four hours. The lengths of the broken parts were found to have contracted in that period to a residual deformation (residual strain relative to original undeformed length) of 2.4 - 2.5. In addition, a set of five samples from the same sheet were stretched at the same rate to strains of 0.25, 0.50, 1.0, 2.0 and 3.0 respectively. The samples were then released and kept at room temperature for twenty-four hours after which time they had all contracted substantially. The corresponding residual deformations were 0.06, 0.12, 0.34, 0.92, and 1.15. The observations will eventually be compared with the behavior of annealed as well as quenched samples treated under similar conditions. Our overall objective is to examine the effect of the crystallinity of UHMWPE on the recovery of the polymer from uniaxial extension, and to determine the nature of the fine structural changes associated with the stretching and recovery processes.

Wide angle and small angle x-ray diffraction methods and scanning electron microscopy will be among the methods used to examine the nature of the permanent and recoverable changes in the fine structure of the UHMWPE caused by uniaxial extension. Information derived from such experiments will also have a bearing on the structural changes which occur in creep, single step stress relaxation, and fatigue experiments.

Initial observations derived from wide angle and small angle x-ray diffraction patterns exhibited by the above mentioned slow cooled samples which were uniaxially stretched at 310K to strains of 1.0, 2.0, and 3.0 and then released are summarized below. As pointed out above the residual strain in these samples after 24 hours at room temperature were 0.34, 0.92 and 1.15 respectively. The wide angle diffraction patterns in Fig. 9 (b,c,d) and the small angle patterns in Fig. 10(a,b,c) were obtained during a period of two to three weeks later. The residual strains were not examined at the times the x-ray patterns were recorded, they were however measured after about eleven weeks and had by then decreased to 0.26, 0.72 and 0.91 respectively. In short, the residual strains in the samples at the time the x-ray patterns were taken were somewhat smaller than 0.34, 0.92 and 1.15, but certainly not less than 0.26, 0.72 and 0.91 respectively. For the sake of brevity in the ensuing discussion of the changes observed in the diffraction patterns with increasing residual strain, we shall identify each of the samples by a two-number code denoting the maximum strain imposed at 310K followed by a bracketed number corresponding to the residual strain after release for 24 hours at room temperature. The manifestation of slow, long term decreases in the residual strain in stretched samples after they are released is a feature which will have to be closely monitored in future studies on the relationship between structural changes and strain.

A wide angle x-ray diffraction pattern from an unstretched slow cooled sheet is shown in Fig. 9a. Figs. 9, b,c,d are diffraction patterns obtained from the 1.0(0.34), 2.0(0.92) and 3.0(1.15) samples respectively. The patterns were recorded with a flat plate camera. Nickel filtered Cu  $K_{\alpha}$  radiation

was used. The x-ray beam was perpendicular to the plane of the gage portion of the deformed dumbbell shaped specimens. The intense 110 and 200 diffraction rings of the common orthorhombic crystalline form of polyethylene are identified in Fig. 9a in which a diffuse halo, H, due to the amorphous regions, can also be seen.

Confining ourselves to the azimuthal changes in the 110 and 200 orthorhombic reflections resulting from stretching, a comparison of the four diffraction patterns shows that as the permanent strain in the samples increases, there is a progressive increase in the intensification of the 200 reflection in the equatorial region. Correspondingly the 110 reflections become broadly split with the most intense portions of the azimuthally broad arcs tending to be closer to the equatorial direction with increasing strain. Somewhat similar observations have been previously reported for lower molecular weight polyethylenes [24,25].

In addition to the changes described above, reflections other than those associated with the usual orthorhombic unit cell of polyethylene were observed in the three stretched samples. The interplanar spacing corresponding to these reflections agreed closely with spacings of 0.456nm, 0.380nm, and 0.355nm<sup>†</sup> which are characteristic of a metastable polymorphic form of polyethylene, which form has been variously described as being triclinic [26] or monoclinic [27]. The indices of the planes having these spacings in the triclinic unit cell proposed by Turner-Jones are (010), (100), and (1 $\bar{1}$ 0) respectively. The corresponding reflections will be identified in what follows as 010<sub>t</sub>, 100<sub>t</sub>, and 1 $\bar{1}$ 0<sub>t</sub>.

<sup>†</sup> These spacings differ from the calculated (110) and (200) interplanar spacings of the orthorhombic unit cell [28] which are 0.41nm and 0.37nm respectively. Among the cases in which these three extra reflections have been previously observed are cold worked samples of polyethylene [29], and samples which were uniaxially extended to a 9.0 strain then annealed at 100°C and subsequently compressed at right angles to the initial stretching direction [27].

The most intense among the extra reflections in the diffraction patterns were the  $010_t$ . They can be seen very clearly in the patterns of the 2.0(0.92) and 3.0(1.15) samples shown in Fig. 9c and Fig. 9d respectively where they appear as arcs whose azimuthal orientations correspond closely to those of the split  $110$  orthorhombic arcs. In comparison, the  $010_t$  reflections are azimuthally much broader in the case of the 1.0(0.34) sample (Fig. 9b) as is the case for the  $110$  orthorhombic reflections. It should be noted that in the diffraction patterns of all three stretched samples the  $010_t$  arcs lie over a diffuse halo associated with the amorphous regions in the specimens.

The  $100_t$  and  $1\bar{1}0_t$  reflections are considerably weaker than the  $010_t$  and are barely if at all visible in Figs. 9b,c,d. They could however be very faintly seen in the original photographic film the  $100_t$  being situated radially between the intense  $110$  and  $200$  orthorhombic reflections but very close to the  $200$ , and the  $(1\bar{1}0)_t$  occurring at a larger radius than the orthorhombic  $200$  arcs. Both the  $100_t$  and  $1\bar{1}0_t$  appeared preferentially arced about the equatorial direction. Whether they were split about that direction could not be determined. Diffraction patterns recorded at larger specimen to film distances may shed some light on this matter.

Small angle x-ray diffraction patterns were recorded from the same samples as those used to obtain the wide angle patterns described above. No diffraction maximum was observed in the unstretched slow cooled sample. This may be attributed to either one of two factors, bearing in mind that the lamellar thickness in melt crystallized polyethylene is in the range 15nm to 90nm, being larger the higher the crystallization temperature. First the equipment used to obtain the diffraction patterns was a small angle camera using pinhole collimation. The upper limit of

thickness measurement with this camera using nickel filtered Cu  $K_{\alpha}$  radiation from a rotating anode source is  $\sim 30\text{nm}$ . It is conceivable that the lamellae in samples slow cooled from 473K to room temperature are thicker than 30nm. Alternatively it may be argued that because the samples are continuously cooled there is a broad distribution in the thickness of the lamellae with the result that no diffraction maximum will be observed even if the lamellar thicknesses are  $< 30\text{nm}$  due to the absence of regularly periodic fluctuations in electron density distribution.

Small angle x-ray diffraction patterns obtained from the 1.0(0.34), 2.0(0.92) and 3.0(1.15) samples are shown in Fig. 10. The main feature exhibited by these patterns is that as the residual strain increases the patterns become four pointed in character (this feature is barely evident in the 1.0(0.34) sample). In addition, the 2.0(0.92) and 3.0(1.15) samples exhibit a central horizontal streak indicating the presence of long and comparatively narrow voids whose long dimension is oriented parallel to the stretching direction. We shall not attempt to discuss these patterns further in this report. They will be examined in the light of the numerous previous small angle x-ray studies carried out on lower molecular weight polyethylenes [see for example references 30-34] subjected to relatively small strains. At present we will simply note that the patterns in Fig. 10b and Fig. 10c indicate that the interfaces between the crystalline and disordered regions in the 2.0(0.92) and 3.0(1.15) samples are appreciably inclined relative to the stretching direction.

(b) Uniaxial Creep.

Uniaxial creep data have been obtained from a set of specimens which were prepared by slow cooling in the press from  $200^{\circ}\text{C}$ . The creep strain versus time is shown in Figure 11 for applied stresses (engineering stress)

in the range from 9 to 27.5MPa. The creep strain was determined with the aid of a cathetometer by monitoring the separation, as a function of time, of marks placed on the gage section of the specimen. The arrow indicates the point at which the specimen stressed at 27.5MPa fractured, and to date represents the only specimen in this set which has failed. At the highest loads the creep strain approaches a maximum and nearly constant value of about 5, whereas at the intermediate and small values of applied load there does appear to be a decrease in the maximum value of strain with decreasing load.

Quenching of the polymer has a significant effect on the creep behavior, as can be seen in Figure 12 which shows a comparison of the creep response for both the quenched and slowly cooled materials. Data are shown for specimens which were subjected to two relatively large applied loads. The principal difference in behavior is that the quenched material creeps much more rapidly initially and then approaches its limiting value of strain much sooner than does the slowly cooled material. Interestingly, in both cases the limiting strain is about the same ( $\approx 5$ ). A difference in crystallinity of about 10% has brought about a quite significant change in the short time creep behavior, while at the same time there is as yet no indication that the failure behavior will be different in the two cases.

### (c) Stress Relaxation

Another method used to characterize the time dependent mechanical behavior of materials is stress relaxation. In this method the specimen is subjected to a constant deformation and the stress is then monitored as a function of time. Such data are presented in Figure 13 for the UHMWPE polymer which was slowly cooled from 200°C. In the present case the specimen was a long strip with straight sides and all the data shown in Figure 13 were obtained from the same specimen. The procedure was as follows.

The specimen was initially subjected to the smallest value of strain shown and the stress monitored for a period of three hours. The specimen was then released and allowed to relax for a period of about 24 hours. The new undeformed length was measured and the next larger step then applied. This procedure was repeated until a strain of about 1.0 was achieved. In the calculation of the true stress, shown as the ordinate in Figure 13, two corrections have been made with respect to the original cross sectional area, one due to the permanent set in the specimen as a result of the prior strain histories, and the other a result of the current step being applied. By permanent set we mean here that fraction of the earlier deformation remaining in the specimen just prior to the application of a new step. For a specimen deformed to a strain of 1.0 the permanent set may be as much as 0.20 or more. If the specimen were allowed to relax for a longer period of time between the application of steps, the recovery would be somewhat greater, and hence the permanent set less. However as a matter of practicality we have chosen as the recovery time a period of about one day.

In Figure 13 it can be seen that up to strains of about 0.35 the rate of relaxation is nearly independent of the level of strain, i.e. the curves are very nearly parallel to one another. This behavior suggests that, to a fair approximation, at small strains the stress,  $\sigma$ , can be represented as the product of a function of time,  $t$ , and a function of strain,  $\epsilon$ , [i.e.  $\sigma(\epsilon, t) = F(\epsilon) \cdot H(t)$ ].

Another representation of the single step stress relaxation data is the one shown in Figure 14 where the data are shown as 120, 960 and 10,000 second isochrones of true stress vs. strain. Hereafter such a representation will be referred to as an (isochronal) stress-strain curve. The points shown as open symbols refer to the data taken from Figure 13. Note that the stress-strain behavior is nonlinear over the entire range of strains examined.

A linear region would be observed in the stress-strain curve only by operating at strains below 0.001. By linear behavior we mean that the modulus is independent of the level of strain and on a log-log plot an isochronal stress-strain curve will be a straight line having a slope of unity. A feature which sets the UHMWPE apart from conventional low molecular weight polyethylenes is that we were able to apply a step in strain as large as 1.0. For linear polyethylenes having molecular weights below 200,000 we have observed that the stress-strain curve flattens at strains above about 0.10. The point at which the curve becomes flat corresponds to a yield point or point at which the material becomes unstable and the phenomenon of necking may occur. For these materials, if one attempts to apply a rapid step in strain to a value larger than about 0.10 the specimen fails. The observation that the UHMWPE does not neck is reflected in Figure 14 by the fact that the stress-strain curve does not flatten but continues to rise at all levels of strain. [Similar data for a specimen which was slowly cooled from 165<sup>o</sup>C rather than 200<sup>o</sup>C are also shown in Figure 14. It is evident that there is no significant difference in the behavior of the two.]

A comparison between the slowly cooled and quenched materials is shown in Figure 15. A significant difference can be seen in stress relaxation behavior between the slow cooled and quenched materials. The isochrones for the quenched material fall well below those for the slowly cooled polymer, and for a given strain the stress (and correspondingly the modulus) is smaller by as much as a factor of two. The isochrones for the quenched material can probably be considered to represent a lower bound for the relaxation behavior of compression molded samples made from the UH-A polymer.

(d) Failure Studies

The failure behavior of UHMWPE is currently being studied under both static (constant loading) and sinusoidal loading conditions. There is a difficulty in conducting time to fail experiments on the UH-A material, because for comparable loading conditions it exhibits a much longer lifetime than do lower molecular weight polyethylenes. Consequently very long testing times are required to collect the desired data, and so far all the data collected have been obtained on specimens subjected to large loads which results in relatively short times to fail (<100 days).

As an aid in analyzing the time to fail data let us first consider an additivity of damage criterion of the type first proposed by Bailey [35]. This criterion is based on the assumption that material failure is a result of damage accumulation due to stress. That is to say, damage which a material experiences as a result of a particular stress history is not recovered, but accumulates in time to some point at which failure occurs. The simple example shown schematically in Figure 16 will serve to demonstrate the idea. Suppose that a material up to time  $t_0$  has a history free of stress. At time  $t_0$ , it is subjected to a stress  $\sigma_0$  for a period of time  $\Delta t_0$ . At time  $t_1$ , it experiences a new stress  $\sigma_1$  for time  $\Delta t_1$ , and so on until at time  $t_n$  a stress,  $\sigma_n$ , is imposed for a period of time  $\Delta t_n$ . The cumulative time of damage or fractional time to failure, is then

$$f(t_n + \Delta t_n) = \frac{\Delta t_0}{\tau_B(\sigma_0)} + \frac{\Delta t_1}{\tau_B(\sigma_1)} + \dots + \frac{\Delta t_n}{\tau_B(\sigma_n)} \quad (1)$$

where the  $\tau_B(\sigma_n)$  are the times to fail for a constant stress  $\sigma_n$ . Note that in the time intervals where the stress is zero there is no contribution to the damage. This means that in the interval from  $t=0$  to  $t=t_1$ , the total damage  $f(t_1)$  is simply  $\Delta t_0 / \tau_B(\sigma_0)$ . However, it should be pointed out

that the same damage could occur if a smaller stress were applied over the entire time interval from  $t=0$  to  $t=t_1$ . This leads to the concept of equivalency of stress histories for which the same total damage occurs. According to the damage criterion, the condition corresponding to failure is  $f(t_n + \Delta t_n) = 1$ .

In integral form the criterion can be expressed as,

$$\int_0^{t_B} \frac{d\xi}{\tau_B[\sigma(\xi)]} = 1 \quad (2)$$

where the integration is carried out over the time variable,  $\xi$ , and  $\tau_B[\sigma(\xi)]$  now represents the time to fail function determined from experiments carried out at constant stress. Each increment in time,  $d\xi$ , is weighted inversely as the lifetime,  $\tau_B(\sigma)$ , which the material would have had under a constant stress  $\sigma$ . The upper limit in the integral is then  $t_B$ , the time to fail for the actual stress history being applied. An advantage of a damage rule of this type is that, in principle, if one can determine the functional form of  $\tau_B(\sigma)$  from constant load experiments, then the lifetime under other loading histories can be predicted from equation (2). For example, in earlier work on lower molecular weight polyethylenes it was found [12,36] that over several decades in time the time to fail behavior could be described by the relationships

$$\tau_B(\sigma) = A e^{-B\sigma} \quad (3)$$

where A and B are constants that depend upon material properties, and  $\sigma$  is the applied stress (engineering stress). For the case where the loading history is sinusoidal

$$\sigma(\xi) = P + Q \sin(\omega\xi) \quad (4)$$

P represents the mean stress and Q the amplitude of the oscillatory component

of stress, and the time to fail is predicted by equation (2) to be

$$t_B = \frac{\tau_B(P)}{I_0(BQ)} \quad (5)$$

where  $\tau_B(P)$  is the time to fail for a constant stress,  $P$ , and  $I_0(BQ)$  the zero order modified Bessel function.

In the case of the lower molecular weight polyethylenes, it was found that for simple loading histories [36] such as those described by equation (1) the damage rule was valid within the experimental error. However, for sinusoidal loading conditions [12] the lifetimes predicted from equation (5) were shorter than the experimentally determined values. Thus for the polyethylenes described in reference [12], the lifetimes predicted using the cumulative damage rule can be considered to represent a lower bound to the actual lifetimes observed experimentally.

Our experience with polymers in general suggests that an important aspect of time dependent failure is the frequency dependence of the fatigue lifetime under sinusoidal loading conditions. One feature of the damage rule described above is that for sinusoidal loading conditions the predicted lifetime is independent of the test frequency, as can be seen from equation (5).

Coleman [37,38] has developed the mathematics of additivity of damage rules for polymer fibers rather extensively. One of the damage rules which he has developed corresponds to the "cycle dependent" fatigue behavior which is often assumed in engineering practice. In cycle dependent fatigue, the damage accumulates due to cycling of the material rather than due to duration under load. In such a case failure would occur after a given number of cycles,  $N_f$ , and the lifetime,  $t_B$ , would vary inversely with test frequency,  $f$ :

$$t_B = \frac{N_f}{f} \quad (6)$$

In the testing of a lower molecular weight polyethylene [12] we have found that neither equation (5) nor equation (6) predicts the lifetime of the material. The prediction from equation (5) is conservative (i.e. observed lifetime is longer than that predicted) while equation (6) greatly overestimates lifetime. This result is of significance in laboratory testing and indicates the importance of determining the frequency dependence of fatigue lifetime. The following illustrates why this is so.

A common assumption in engineering practice is that fatigue failure is a cycle dependent phenomenon, not a time dependent one. As a result, common laboratory practice calls for "accelerating" fatigue tests by increasing the test frequency, counting the number of cycles to failure and using this number as a measure of the fatigue resistance of the material. Thus, for example, if an "accelerated" test at 35Hz were to determine that the lifetime of a UHMWPE component is  $10^8$  cycles, then the expected in vivo lifetime (assuming a frequency of 1 Hz) would also be  $10^8$  cycles, or 3 years. If, however, the time to fail of the material were independent of test frequency, as predicted by equation 5, then the lifetime at 35 Hz of  $10^8$  cycles would correspond to a lifetime of  $2.9 \times 10^6$  cycles at 1 Hz or a time to fail of only 33 days.

The failure criteria described above then provide a useful framework within which to consider the time dependent failure behavior of UHMWPE. We have chosen to study two important aspects of material failure, namely:

- (1) The time to fail behavior under both static and cyclic loading conditions.
- (2) The dependence of the time to fail on test frequency under cyclic loading.

Our results to date for specimens failed at constant load (creep data) and in zero-tension sinusoidal loading at 0.002 Hz (fatigue data) are shown in

Figure 17. The solid and dashed lines represent linear regression curves of the form given by equation (3). It should be pointed out that these curves are based on relatively few data points which exhibit considerable scatter (unlike the lower molecular weight polyethylenes [12,36] which show very little scatter in the time to fail data). The data indicate that the fatigue lifetimes under sinusoidal loading are approximately 6-7 times greater than the static lifetimes. This result is in close agreement with the fatigue lifetime predicted from equation (5) using the regression equation fitted to the creep data.

We are also in the process of doing fatigue experiments at 0.0002 and 0.01 Hz to investigate the effect, if any, of test frequency on the material lifetime. Preliminary results do not show any clear trend toward a dependence of lifetime on frequency.

A comment is in order concerning the choice of frequencies used in this study to characterize the fatigue behavior of UHMWPE. We have chosen test frequencies in the 0.0002 to 0.01 Hz range, whereas in the clinical environment frequencies in the 1 Hz range are more typical. In order to conduct fatigue tests within an acceptable length of time it is necessary to carry out the testing at relatively high levels of stress. At such stress levels the amount of hysteretic heating can be substantial, thus greatly biasing the test results. We have therefore chosen somewhat lower frequencies in order to assure that the tests are conducted under nominally isothermal conditions.

(e) Equal-Biaxial Deformations Under Inflation and Environmental  
Stress Cracking

Work in these areas has just begun. The disc inflation apparatus used to achieve equal-biaxial deformation histories is shown schematically in

Figure 17. A sheet of material is clamped as shown and a constant pressure is then applied to one side of the specimen. The deformation is equal-biaxial only in the immediate vicinity of the pole. The true stress at the pole can be calculated for a given stretch using the following relationship [39]:

$$\sigma = \frac{p}{2} \frac{r}{h} \lambda^2 \quad (7)$$

where  $\sigma$  is the true stress,  $p$  is the applied pressure,  $r$  is the radius of curvature measured at the pole,  $h$  is the initial thickness of the sheet, and  $\lambda$  is the stretch determined at the pole.

The environmental stress-crack resistance of the UHMWPE is being investigated by two methods. In one method a small amount of the stress-cracking agent (in the present case a ten percent solution of nonylphenoxy-poly(ethyleneoxy) ethanol in distilled water) is introduced into the inflation apparatus prior to pressurization. As soon as the apparatus is pressurized it is inverted so that the liquid is in contact with the specimen only in the region near the pole.

In the second method a test being developed for ASTM Committee D-20.10 on plastics is used. This test is based on a bent strip geometry. These tests are performed at different temperatures in the 333 to 393K range.

Unlike low molecular weight polyethylenes the lifetime of the UHMWPE in stress cracking agent is extremely long. For example, one sheet of the UHMWPE being tested in the inflation apparatus at a pressure of 0.48 MPa (70 PSI) has not failed in nearly seven months whereas a similar sheet of a low molecular weight polyethylene failed almost immediately. Thus far, none of the specimens being tested either in air or in stress-cracking agent, by either method, has failed. It appears that the pressurizing

system for the inflation apparatus will have to be redesigned in order to operate at higher pressures, or alternatively the tests will have to be carried out at higher temperatures.

(f) Miscellaneous

In the Second Quarterly Report [40] we compared the creep behavior of the UHMWPE polymer used in the present study to that of specimens molded from another batch of UHMWPE polymer (UH-B) obtained from the same manufacturer several years earlier. It was noted that the creep compliance and time to failure behavior was quite different for the two materials even though the intrinsic viscosities of the raw polymers and densities of the molded sheets were essentially the same. The specimens made from the two batches of polymer were, however, molded under different conditions. The molding temperature was 473K (200°C) for the UH-A polymer and it was 428K (155°C) for the UH-B. Since then we have prepared molded sheets from the UH-B polymer using the same molding (473K) and slow cooling procedure outlined in Section 2. The creep and stress relaxation data were within 5% of the values for the UH-A material presently being used. The greater creep compliance and shorter time to fail exhibited by the UH-B specimens molded at 428K can be reasonably attributed to poor interparticle adhesion at the lower molding temperature.

#### 4. Summary

Work carried out in FY 1980 consisted of two phases, the first of which was concerned with the preparation of compression molded sheets of UHMWPE suitable for studying the mechanical properties of the polymer. Features of the fine structure of the raw polymer as well as of the compression molded sheets were also examined. In the second phase investigations were started on various aspects of the mechanical properties of UHMWPE, namely stress-strain behavior at constant rate of clamp separation, creep and single step stress relaxation in uniaxial extension, and failure under both static and sinusoidal loading conditions. A study of fine structure changes resulting from uniaxial deformation under constant rate of clamp separation has also been started. In addition, preliminary work was done on the equal biaxial deformation (under inflation) and the stress crack resistance of UHMWPE.

Three aspects of the raw polymer have been examined, its morphological characteristics, its melting behavior, and its crystallinity. The polymer, as received, is in its as-polymerized state and consists of fine particles. Because of its very high melt viscosity both molded and machined prothesis components made from it retain a memory of the particulate nature of the raw polymer. This was also true for specimens molded in our laboratory at temperatures as high as 90K above the melting point. This observation emphasizes the importance of characterizing the structure of UHMWPE products, not only to determine their crystallinity, but also to monitor those aspects of their morphology which are directly related to, and a consequence of, the particulate nature of the raw polymer. Since the nature of the shapes, sizes, and fine textures of nascent polyethylene particles vary depending upon the polymerization conditions, knowledge of the morphology of the raw polymer is a necessary aspect of the present study.

The raw polymer particles were examined in a scanning electron microscope. The particles, which are irregularly shaped, and which differ in size in the range  $80\mu\text{m} - 300\mu\text{m}$ , exhibit at low magnifications an external appearance resembling that of compact clumps of grapes. Examination at high magnifications revealed regions which were highly porous. The voids in these regions were bridged by microfibrils,  $50\text{nm} - 100\text{nm}$  in diameter, which probably result from the deformation of the polymer during polymerization as a consequence of the progressive expansion of the particles caused by the continued generation of fresh polymer at the surface of underlying encapsuled catalyst.

Differential scanning calorimetry (DSC) was used to examine the melting behavior and crystallinity of the raw polymer. The melting point was found to be between  $413$  and  $414\text{K}$  ( $140-141^{\circ}\text{C}$ ). The percent crystallinity, as determined from the area under the melting curve, was  $78\%$ , which represents a value significantly higher than can be expected for the same material compression molded at temperatures above the melting point.

Considerable time was devoted to the design and construction of vacuum molding equipment and to the establishment of procedures for molding laboratory specimens of the UHMWPE. Protocols were established for preparing compression molded sheets having weight % crystallinities of close to either  $50\%$  or  $60\%$  (densities close to  $0.923\text{ g/cm}^3$  or  $0.936\text{ g.cm}^3$ ) by respectively rapidly cooling or slowly cooling polymer melted at  $473\text{K}$ .

Examination of cross-sections of the sheets under a light microscope using phase contrast optics revealed the retention of a memory of the original particulate nature of the raw polymer in the sheets. Examination of cross-sections of the slow cooled sheets under a polarizing light microscope showed that there was a wide variation in the sizes of the birefringent structures in them. The larger among these structures appeared to be axialitic or spherulitic

in character. Retention of a memory of the raw polymer particles and the wide variation in the sizes of the birefringent structures were also observed in sheets compression molded at 503K.

The deformation and failure of slow cooled ( $\rho=0.936 \text{ g/cm}^3$ ) samples of UHMWPE subjected to uniaxial extension have been examined in constant rate of clamp separation, creep, stress relaxation, and sinusoidal loading experiments. Only the creep and stress relaxation characteristics of rapidly cooled samples ( $\rho=0.923 \text{ g/cm}^3$ ) have been examined so far.

Constant rate of clamp separation experiments were carried out on slow cooled samples at 296K and 310K at clamp separation rates in the range 0.02 in./min. to 2.0 in./min. Both the modulus and the strength at break decreased with decreasing rate of deformation and with increasing temperature as is the case for for lower molecular weight linear polyethylenes. In contrast with the behavior of the lower molecular weight polyethylenes the slow cooled sheets of UHMWPE did not exhibit the phenomenon of necking. The specimens underwent uniform drawing along their length up to the point of failure. Constant rate of clamp separation experiments on slow cooled samples were also carried out in which specimens were stretched to various predetermined strains below the breaking strain and were then released. These specimens, which exhibited substantial recovery from the imposed strain, are being used as models for the study of the morphological changes associated with the deformation of UHMWPE. A preliminary examination of such specimens has been carried out using wide angle and small angle x-ray diffraction.

Stress relaxation and creep experiments have been carried out at 296K on both slow cooled and quenched samples. Although the crystallinities of these samples (~60%, ~51% respectively) differed by only ~10%, there were significant differences between their stress relaxation behaviors and between their creep

behaviors. At strains ranging from 0.001 to 1.0 and over times from 60s to 10,000s the relaxation modulus of the slow cooled samples was approximately twice as large as that of the rapidly quenched ones. In the creep experiments the slow cooled samples exhibited a much greater resistance to creep than the quenched ones during the early stages of deformation. The limiting creep elongation (strain at failure), however, was approximately the same (~5) for both types of samples.

## 5. Work Plan for FY 1981

The work described in this report represents the initial stages of a project concerned with the characterization of the morphology and mechanical behavior of UHMWPE. In particular we are interested in, (1) determining the influence of processing conditions (thermal history) on the morphology and mechanical behavior of UHMWPE and (2) studying the changes in morphology which result from mechanical deformation. During FY 1980 we concentrated our efforts on developing molding apparatus and procedures for producing sheets of UHMWPE which are suitable for preparation of specimens for uniaxial (dumbbell, strip) and equal biaxial (circular sheets) test specimens. In addition considerable effort was spent in characterizing the morphology and mechanical behavior of UHMWPE, which was slowly cooled from the melt. The experiments, to characterize the mechanical behavior of UHMWPE have been largely carried out at room temperature and in uniaxial extension.

During FY 1981 the work presented in this report will be extended to obtain additional data at room temperature. In addition, work will be initiated to study the mechanical behavior of UHMWPE at higher temperatures and in other modes of deformation. The following outlines the work which is proposed for FY 1981.

1. Experimental work begun in the areas of uniaxial creep, stress relaxation and static and dynamic fatigue will be continued and extended to higher temperature [310K (37°C)]. The creep behavior will be characterized in 0.15N saline solution as well as laboratory air. In addition, the effect of morphology as changed by varying specimen fabrication procedures (quenching, annealing, etc.) on mechanical behavior will continue to be examined.

2. Work already initiated to study the equal biaxial creep behavior and stress crack resistance of UHMWPE will be continued. Because of the long lifetime of UHMWPE in stress-cracking fluid the stress crack tests will be carried out at elevated temperatures.
3. Experiments will be initiated to study the compressive creep and compressive stress relaxation behavior of UHMWPE. Initial work will involve the development of apparatus and procedures for compression molding cylinders of UHMWPE.
4. The use of specimens deformed under uniaxial testing conditions as a model for studying morphological changes associated with deformation will continue. This work will be extended to examine features associated with creep and cyclic loading of the polymer in addition to the constant rate of elongation experiments examined in FY 1980.

Appendix A

The percent crystallinity of polyethylene can be determined either from density measurements or from Differential Scanning Calorimetry (DSC). In the present work the density was determined with a water-ethanol density gradient column at 296.3K. The weight percent crystallinity is calculated with the following equation,

$$\chi \text{ (percent crystallinity)} = \frac{\rho_c}{\rho} \frac{(\rho - \rho_a)}{(\rho_c - \rho_a)} \chi 100 \quad (1)$$

where  $\rho$  is the measured density of the polymer,  $\rho_a$  is the density of the amorphous polyethylene, and  $\rho_c$  is the density of a polyethylene crystal. In the present instance values of  $\rho_a = 0.855 \text{ g.cm}^3$  [41] and  $\rho_c = 1.0 \text{ g.cm}^3$  [28] were used.

The percent crystallinity, as determined from DSC, is defined by the following relationship.

$$\chi = \frac{\Delta H}{\Delta H_0} \quad (2)$$

where  $\Delta H$  is the heat of fusion determined from the area under the melting peak and  $\Delta H_0$  is the heat of fusion for a purely crystalline specimen. In the present case a value of 71.43 cal/g was used for  $\Delta H_0$  [40].

$\Delta H$  is determined with the following equation:

$$\Delta H = 0.2614 \frac{RAK}{WS} \text{ cal/g.}$$

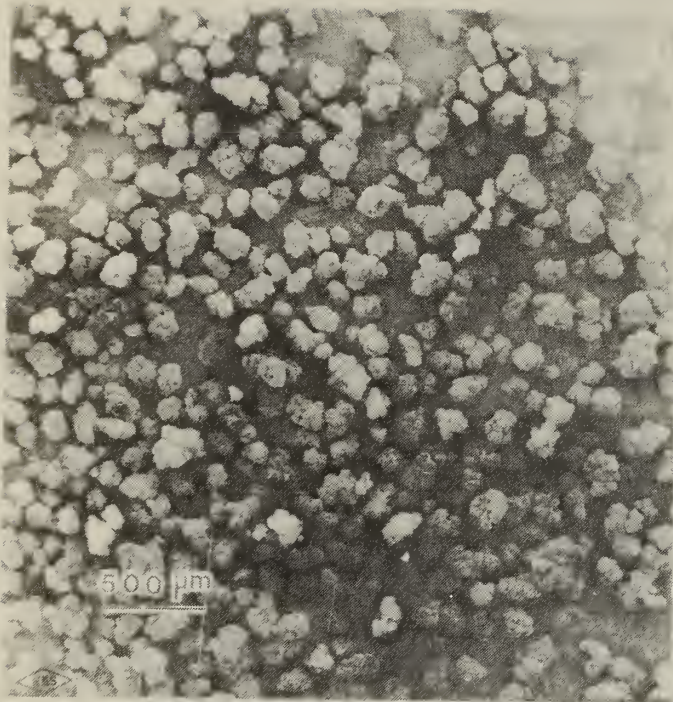
where R = heating rate (m cal/°c)  
A = area under the melting peak (mm<sup>2</sup>)  
K = a calibration constant  
W = mass of the specimen (mg)  
S = recorder speed (mm/min)

References

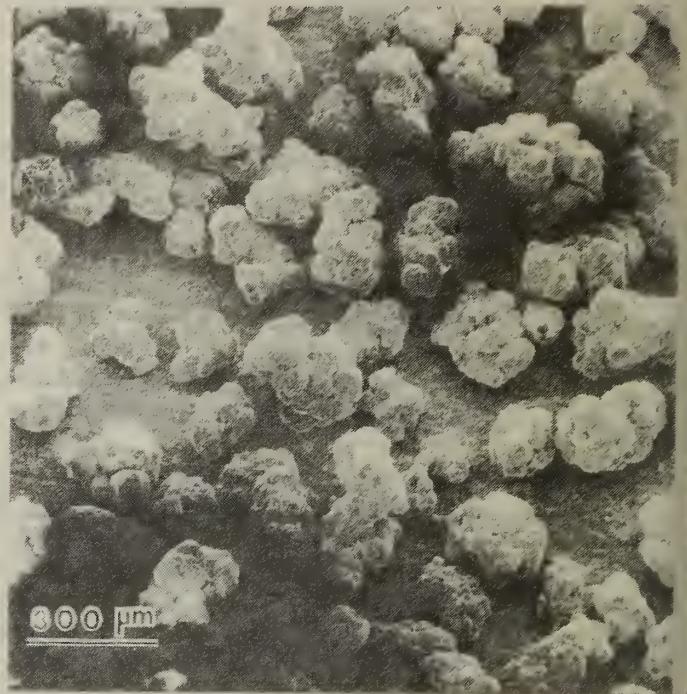
1. J. M. Dowling, J. R. Atkinson, D. Dowson, and J. Charnley, "The Characteristics of Acetabular Cups Worn in the Human Body", *J. Bone Joint Surg.*, 60-B(3), 375 (1978).
2. J. R. Atkinson, K. J. Brown and D. Dowson, "The Wear of High Molecular Weight Polyethylene. Part I", *J. Lubrication Technology*, 100(2), 208 (1978).
3. E. A. Salvati, T. M. Wright, A. H. Burstein, and B. Jacobs, "Fracture of Polyethylene Acetabular Cups", *J. Bone Joint Surg.*, 61-A(8), 1239 (1979).
4. B. Weightman, D. P. Isherwood and S. A. V. Swanson, "The Fracture of Ultrahigh Molecular Weight Polyethylene in the Human Body", *J. Biomed. Mater. Res.*, 13, 669 (1979).
5. P. D. Ritchie, ed. Physics of Plastics, Iliffe Books, Ltd., London, 1965.
6. F. W. Bilmeyer, Jr., Textbook of Polymer Science, Interscience Publishers, New York, 1966.
7. F. Khoury, H. L. Wagner, L. J. Zapas, and J. P. Colson, "Aspects of the Characterization of Ultra High Molecular Weight Polyethylene", paper presented at the Ninth International Biomaterials Symposium, New Orleans, 1977.
8. D. F. Gibbons, J. M. Anderson, R. L. Martin and T. Nelson, "Wear and Degradation of Retrieved Ultra High Molecular Weight Polyethylene and Other Polymeric Implants", *Corrosion and Degradation of Implant Materials*, ASTM STP684, B. C. Syrett and A. Acharya Eds., ASTM 1979, pp 20-40.
9. S. K. Bhateja, J. K. Rieke and E. H. Andrews, "Impact Fatigue Response of Ultra-High Molecular Weight Linear Polyethylene", *J. Matls. Sci.*, 14, 2103 (1979).
10. R. M. Rose, A. Crugnola, M. Ries, W. R. Cimino, I. Paul, and E. L. Radin, "On the Origins of High In Vivo Wear Rates in Polyethylene Components of Total Joint Prostheses", *Clinical Orthopedics and Related Research*, 145, 277 (1979).
11. J. M. Crissman and L. J. Zapas, "Creep Failure and Fracture of Polyethylene in Uniaxial Extension", *Polym. Eng. and Sci.*, 19, 99 (1979).
12. G. B. McKenna and R. W. Penn, "Time Dependent Failure of Poly(methyl methacrylate) and Polyethylene", *Polymer*, 21, 213 (1980).
13. J. K. Lancaster, "Basic Mechanisms of Friction and Wear of Polymers", *Plastics and Polymers*, 297 (Dec. 1973).

14. P. S. Walker, "The Measurement and Effects of Friction and Wear in Artificial Hip Joints", J. Biomed. Mater. Res. Symposium, 4, 327 (1973).
15. B. O. Weightman, I. L. Paul, R. M. Rose, S. R. Simon and E. L. Radin, "A Comparative Study of Total Hip Replacement Prostheses", J. Biomechanics, 6, 299 (1973).
16. H. L. Wagner and J. G. Dillon, "A Specification Method for Ultra High Molecular Weight Polyethylene for Implant Use", J. Biomed. Mater. Res., 13, 821 (1979).
17. R. H. Marchessault, B. Fisa, and H. D. Chanzy, "Nascent morphology of polyolefins", Crit. Rev. Macromol. Sci. 1, 315 (1972).
18. B. Wunderlich, "Macromolecular Physics, Vol. 2", Academic Press, N.Y. 1976, see pp 282-293.
19. For a discussion of the equilibrium melting point of polyethylene see for example, J. D. Hoffman, G. T. Davis, and J. I. Lauritzen Jr., "The Rate of Crystallization of Linear Polymers with Chain Folding", Chapter 7 (see page 567), in Treatise on Solid State Chemistry Vol. 3, N. B. Hannag Ed., Plenum Press N.Y. (1976).
20. J. D. Hoffman, G. S. Ross, L. Frolen and J. I. Lauritzen, Jr., "On the growth Rate of Spherulites and Axialites from the Melt in Polyethylene Fractions: Regime I and Regime II Crystallization", J. Res. Nat. Bur. Stds. (U.S.), 79A, 671 (1975).
21. J. Maxfield and L. Mandelkern, "Crystallinity, Supermolecular Structure and Thermodynamic Properties of Linear Polyethylene Fractions", Macromolecules, 10, 1141 (1977).
22. F. Khoury and E. Passaglia, "The Morphology of Crystalline Synthetic Polymers", in Treatise on Solid State Chemistry, N. B. Hannay ed. (Plenum Press, New York), Vol. 3, 335 (1976). (See pp 466-472).
23. H. J. Nusbaum and R. M. Rose, "The Effects of Radiation Sterilization on the Properties of Ultra High Molecular Weight Polyethylene", J. Biomed. Mater. Res. 13, 557 (1979).
24. I. L. Hay and A. Keller, "Polymer Deformation in Terms of Spherulites", Kolloid Z. u Z. Polymere, 204, 43 (1965).
25. A. Keller, "Unusual Orientation Phenomena in Polyethylene Interpreted in Terms of the Morphology", J. Polymer Sci. 15, 31 (1955).
26. A. Turner Jones, "The Triclinic Crystal Form of Polymethylenes and Polyethylene", J. Polymer Sci., 62, 553 (1962).
27. K. Tanaka, T. Seto, and T. Hara, "Crystal Structure of a New Form of High Density Polyethylene", J. Phys. Soc. Japan, 17, 873 (1962).

28. C. W. Bunn, "The Crystal Structure of long-chain paraffin hydrocarbons. The shape of the CH<sub>2</sub> group", Trans. Faraday Soc. 39, 482 (1939).
29. P. W. Teare and D. R. Holmes, "Extra Reflections in the X-ray Diffraction Pattern of Polyethylenes and Polymethylenes", J. Polymer Sci. 24, 496 (1957).
30. N. Kasai and M. Kakudo, "Fine Texture in Necking Portions of Cold-Drawn Polyethylene", J. Polymer Sci. A 2, 1955 (1964).
31. R. Corneliussen and A. Peterlin, "The influence of Temperature on the Plastic Deformation of Polyethylene", Makromol. Chem. 105, 193 (1967).
32. V. A. Marikhin and L. P. Myasinkova, "The Role of Interfibrillar Tie Molecules in Drawing of Polymers", J. Polymer Sci: Polymer Symp. 58, 97 (1977).
33. P. B. Bowden and R. J. Young, "Deformation Mechanisms in Crystalline Polymers", J. Matls. Res. 9, 2034 (1974).
34. L. E. Alexander, "X-ray Diffraction Methods in Polymer Science", Wiley-Interscience, New York (1969).
35. J. Bailey, "An attempt to Correlate Some Tensile Strength Measurements on Glass: III", Glass Industry, 20, 94 (1939).
36. J. M. Crissman, C. M. Guttman, and L. J. Zapas, "Performance of Plastic Packaging for Hazardous Materials Transportation. Part I: Mechanical Properties", Report No. DOT/MTB/OHMO-76/4, October, 1976.
37. Coleman, B.D. "Application of the Theory of Absolute Reaction Rates to the Creep Failure of Polymeric Filaments", J. Polymer Sci., 20, 447(1956).
38. Coleman, B. D., "Statistics and Time Dependence of Mechanical Breakdown in Fibers", J. Appl. Phys. 29, 968 (1958).
39. J. E. Adkins and R. S. Rivlin, "Large Elastic Deformations of Isotropic Materials: IX. The Deformation of Thin Shells", Phil.Trans.Royal Soc. London, A244, 505 (1952).
40. G. B. McKenna, F. Khoury and J. M. Crissman, Second Quarterly Report Jan.-April, 1980, Task 80-01, NBS-BMD Interagency Agreement.
41. G. T. Davis and R. K. Eby, "Glass Transition of Polyethylene: Volume Relaxation", J. Appl. Phys, 44, 4274 (1973).
42. M. G. Broadhurst, "Thermodynamic Properties of Polyethylene Predicted from Paraffin Data, J. Research Natl. Bur. Std. 67A, 233 (1963).



a



b

Fig. 1 Scanning electron micrographs illustrating the particles of raw ultra high molecular weight polyethylene UH-A at two different magnifications.

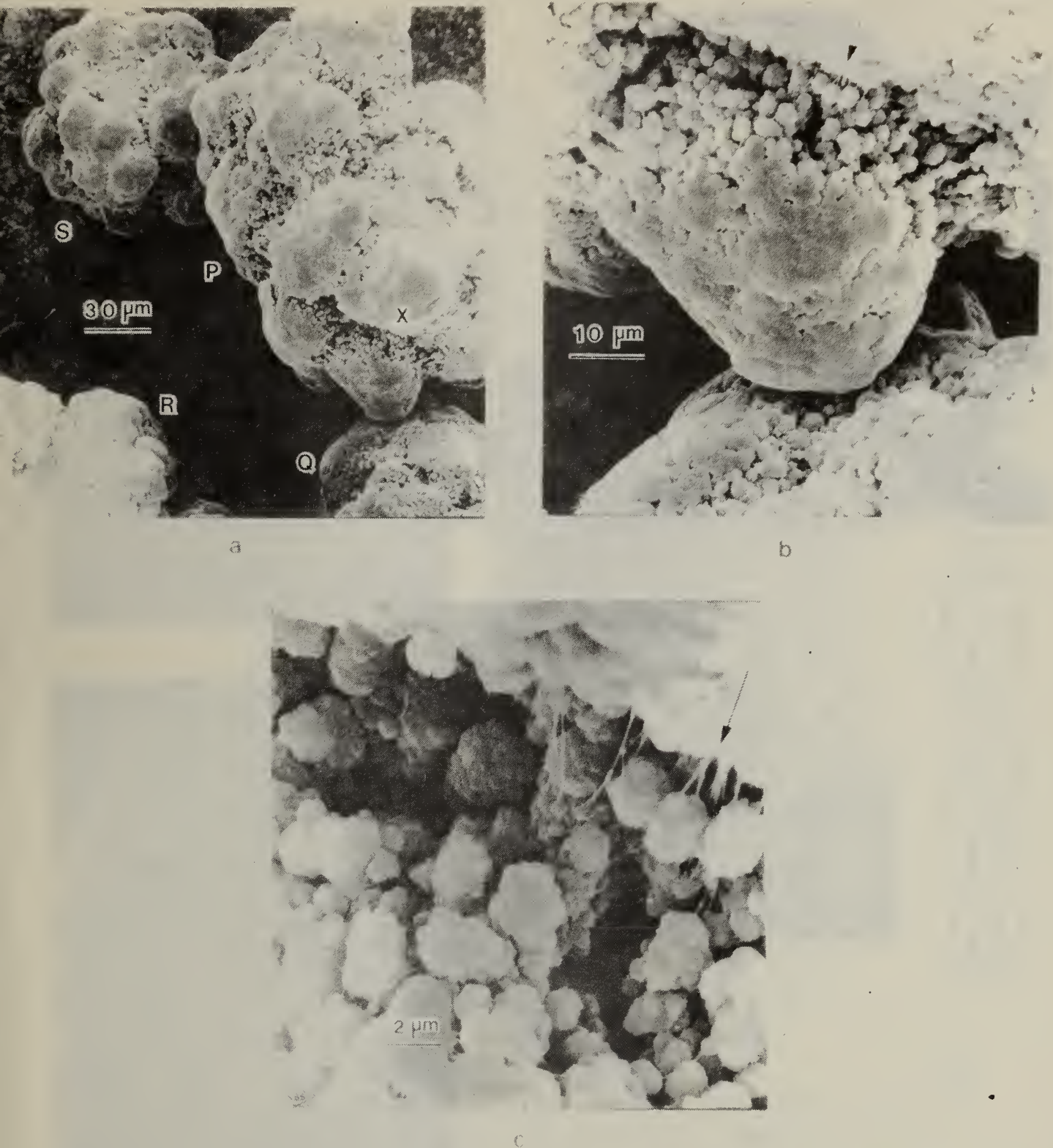


Fig. 2 Scanning electron micrograph showing particles P,Q,R,S of raw UH-A polymer. The region below that marked X of particle P in (a) is shown a two higher magnifications in (b) and (c) respectively. Note the fibrils in (b) and (c) in which the arrows identify the same region in both pictures.



a



b

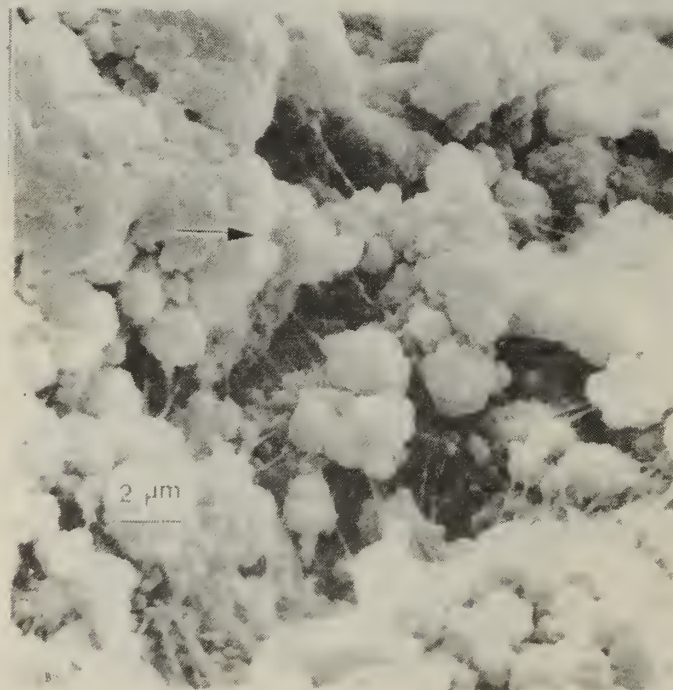


Fig. 3 (a) Scanning electron micrograph of a particle of raw UH-A polymer. The region to the right of the area Y is shown at two higher magnifications in (b) and (c) respectively. Note the fibrils in (b) and (c) in which the arrows identify the same region in both pictures.

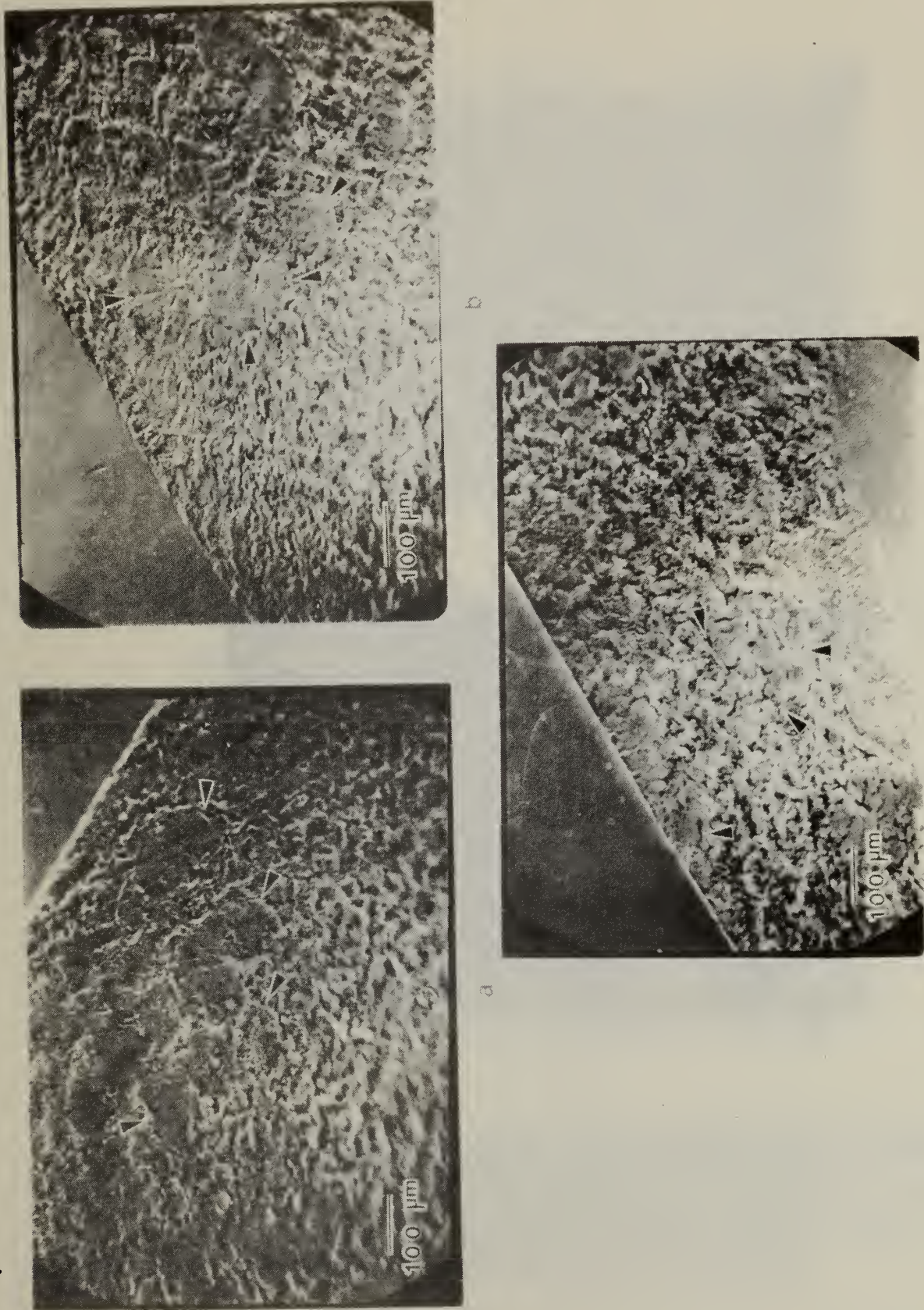


Fig. 4 Low magnification micrographs taken in a light microscope (using transmission phase contrast optics) showing cross-sections of slow cooled sheets of UH-A polymer compression molded at (a) 463K, (b) 473K and (c) 503K. Markers point to some of the boundaries between the original raw polymer particles.

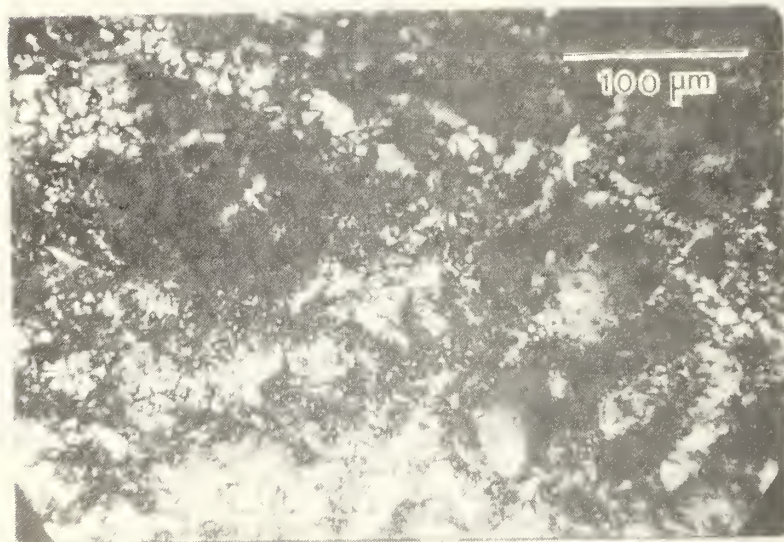
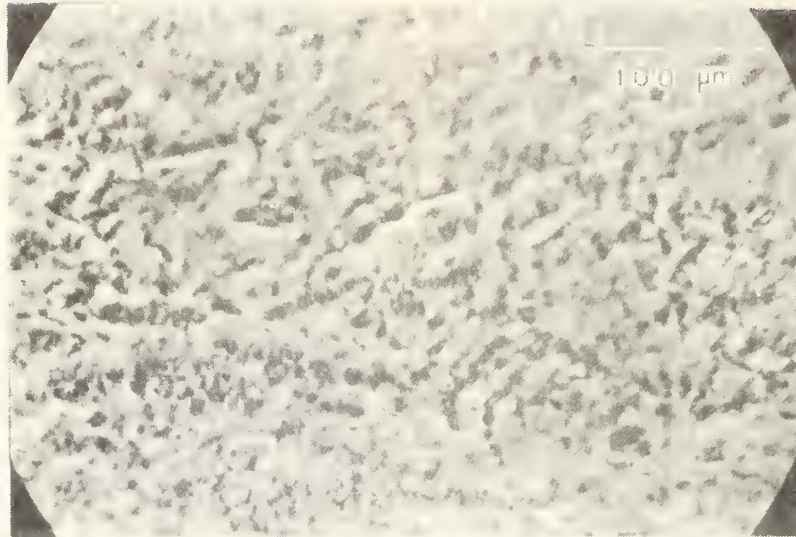
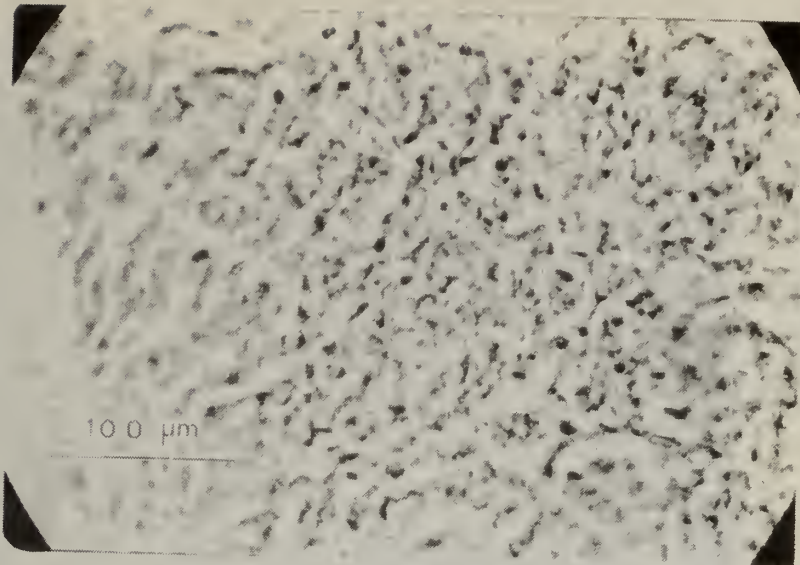


Fig. 5 Light micrographs of an area in a cross-section of a sheet of UH-A polymer molded at 463K, (a) Phase contrast optics, (b) crossed polarizer and analyzer. Note the variation in the sizes of the birefringent structures in (b). The fine variations in contrast in (a) are associated with the birefringent structures in the sample.



a



b

Fig. 6 Light micrographs of an area in a cross-section of a sheet of UH-A polymer molded at 473K. (a) Phase contrast optics, (b) crossed polarizer and analyzer. Note the variation in the sizes of the birefringent structures in (b). The fine variations in contrast in (a) are associated with the birefringent structures in the sample.

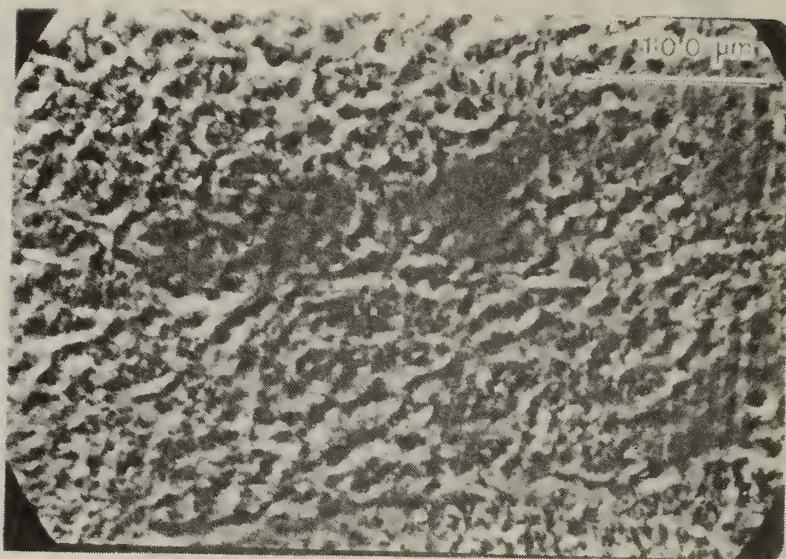


Fig. 7 Light micrographs of an area in a cross-section of a sheet of UH-A polymer molded at 503K. (a) Phase contrast optics, (b) crossed polarizer and analyzer. Note the variation in the sizes of the birefringent structures in (b). The fine variations in contrast in (a) are associated with the birefringent structures in the sample.

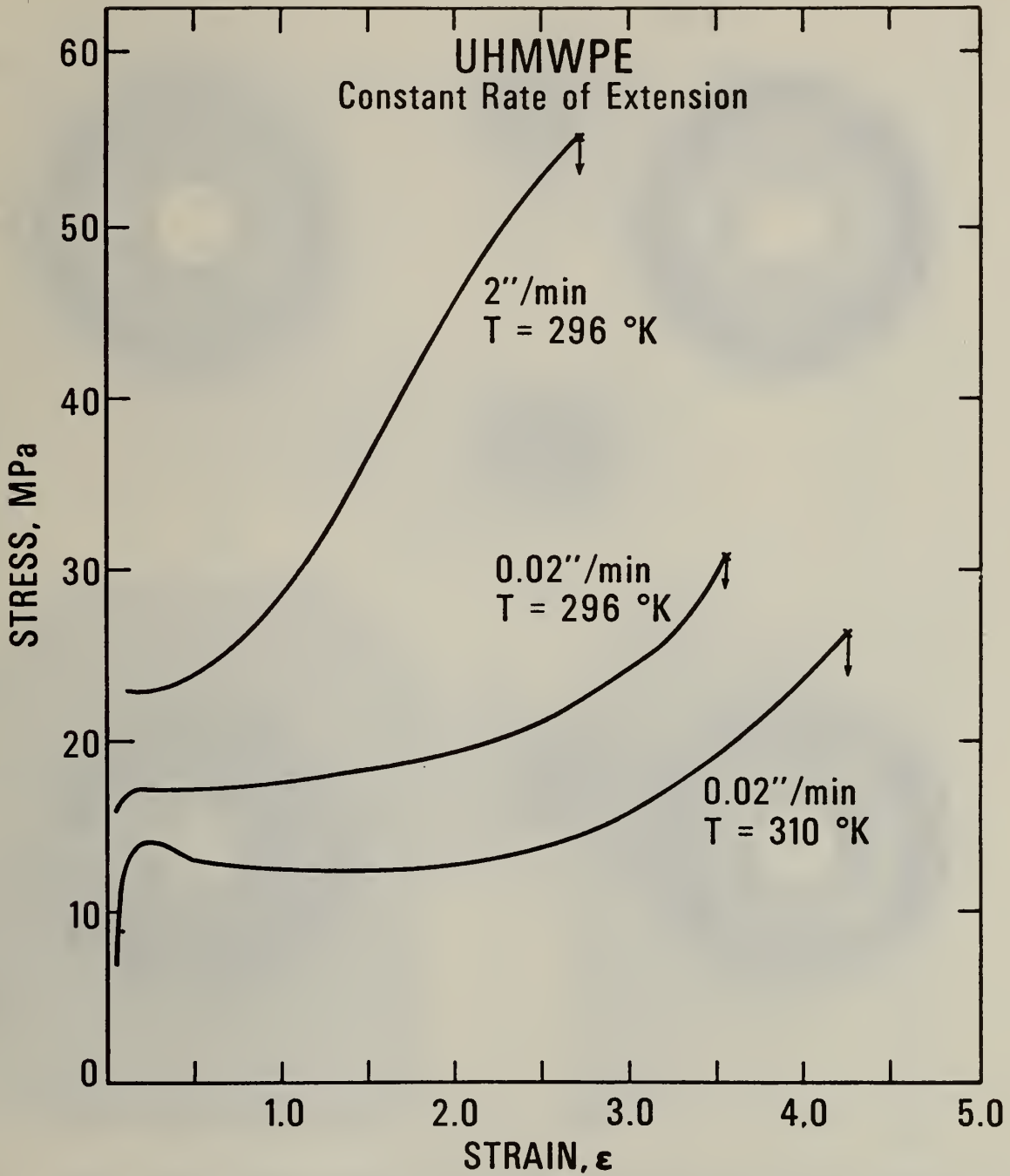


Fig. 8 Engineering stress versus strain for specimens of UHMWPE elongated at different rates of clamp separation. UH-A slowly cooled from 473K (200°C).

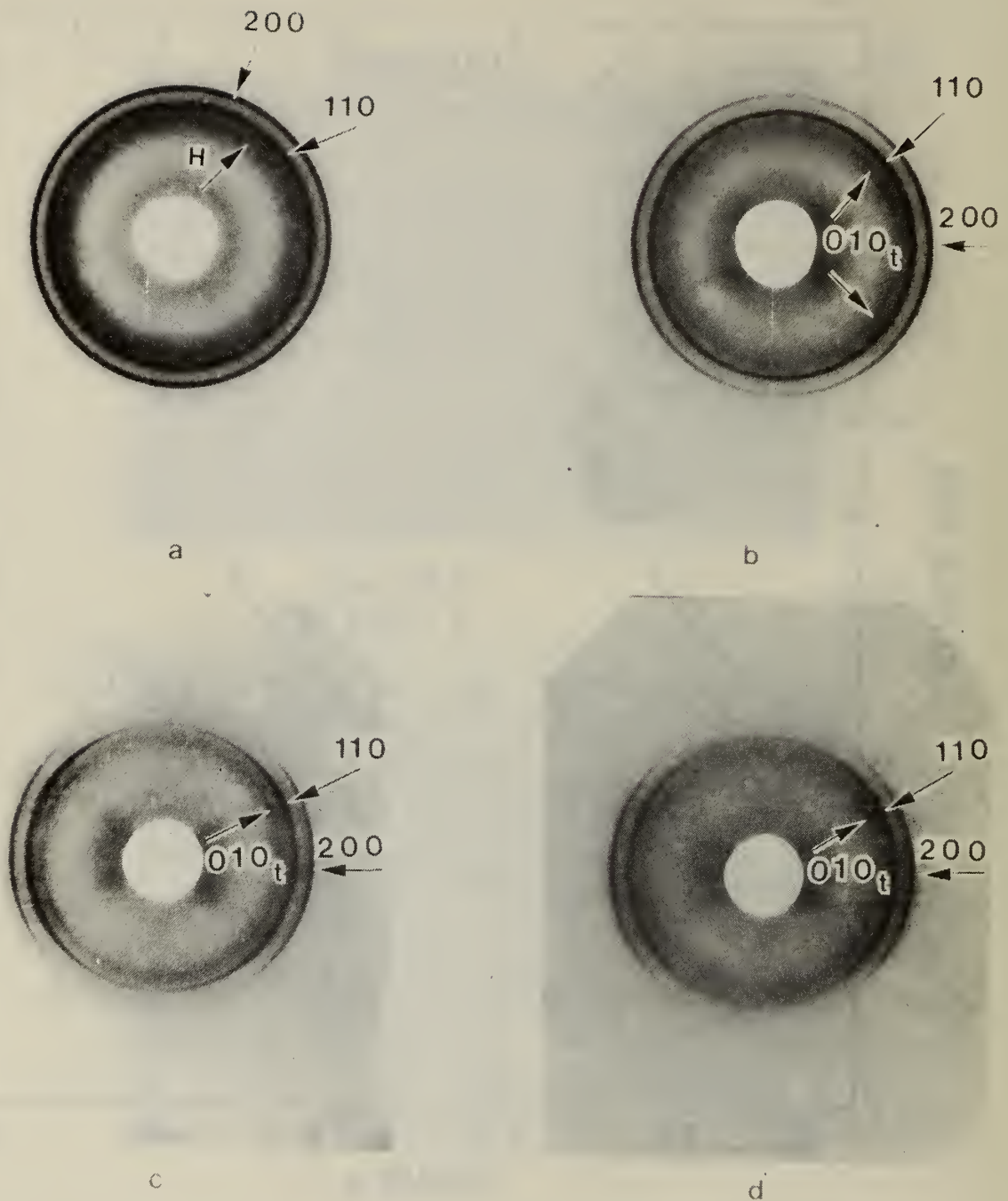


Fig. 9 (a) Wide angle x-ray diffraction pattern from an unstretched sheet of UH-A which was molded at 473K and then slow cooled. The other diffraction patterns were exhibited by specimens (from the same sheet) which had been stretched at 310K (37°C) to strains of (b) 1.0, (c) 2.0 and (d) 3.0, and then released and stored at room temperature. The residual strains in the specimens after storage at room temperature for twenty-four hours were 0.34, 0.92, and 1.15 respectively. The corresponding residual strains after eleven weeks were 0.26, 0.72 and 0.92. The diffraction patterns were recorded about two to three weeks after stretching (see text). Stretching direction vertical. Letter H in (a) denotes 'amorphous' halo. Reflections  $010_t$  are associated with the triclinic crystal form [26] of polyethylene.



a



b



c

Fig. 10 Small angle x-ray diffraction patterns from the same stretched specimens as those used to obtain the wide angle patterns in Fig. 9b, 9c and 9d. The specimens were originally stretched at 310K to strains of (a) 1.0, (b) 2.0, and (c) 3.0. The residual strains in the specimens after they were released and stored at room temperature for 24 hours were 0.34, 0.92 and 1.15 respectively. The corresponding residual strains after eleven weeks were 0.26, 0.72 and 0.92. The diffraction patterns were recorded about two to three weeks after stretching (see text). Stretching direction vertical. (Specimen to film distance 52cm; magnification of photographs compared to original film X1.5).

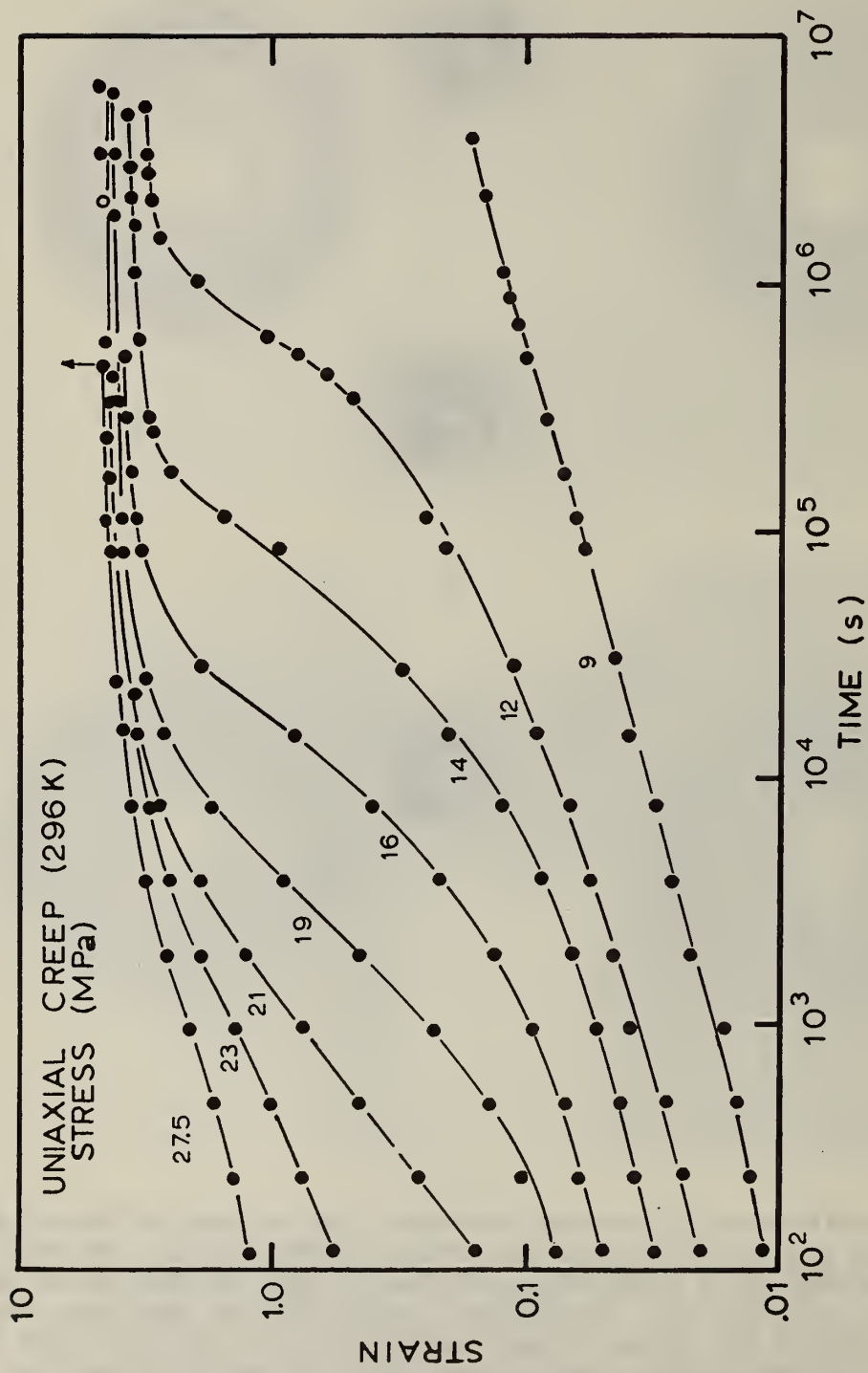


Fig. 11 Uniaxial creep for specimens of UHMWPE (UH-A) slowly cooled from 473K (200°C). The engineering stress is indicated by the numbers shown.

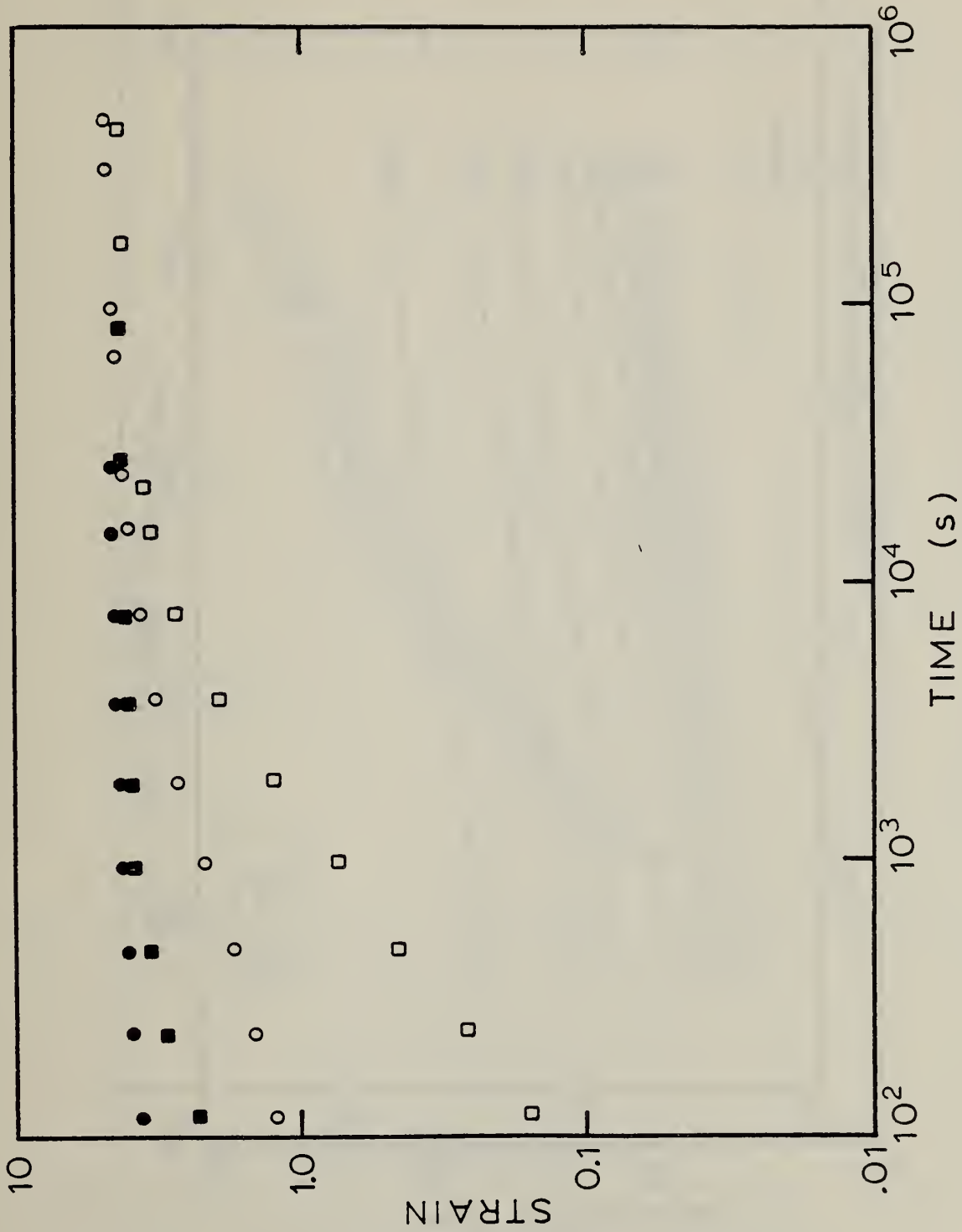


Fig. 12 Comparison of uniaxial creep for specimens of UHMWPE (UH-A) slowly cooled and quenched from 473K (200°C). Open symbols - slowly cooled, filled symbols - quenched; circles - 27.5 MPa, squares - 21 MPa engineering stress.

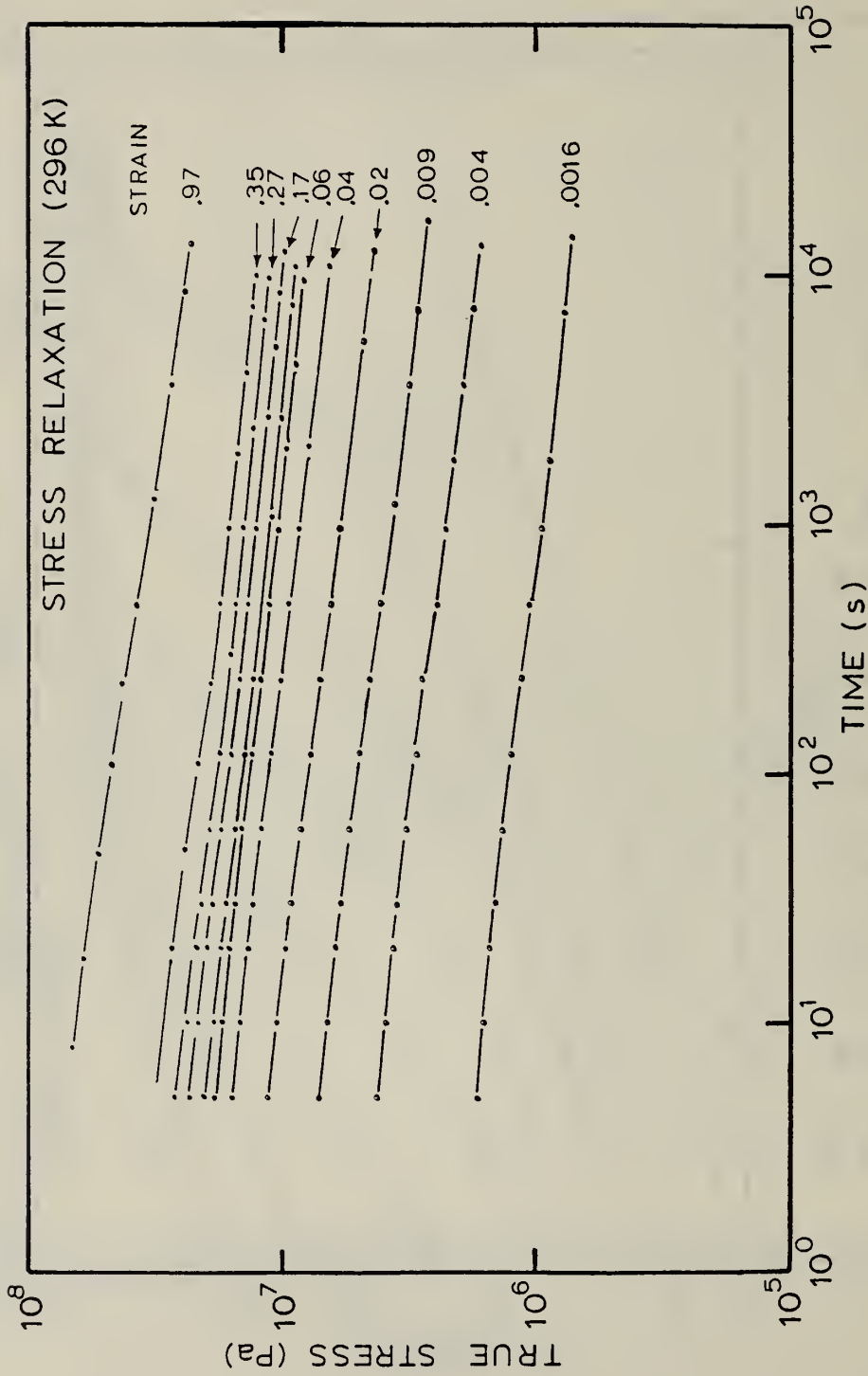


Fig. 13 True stress versus time for UHMWPE (UH-A) slowly cooled from 473K (200°C). The data were obtained from single step stress-relaxation experiments carried out on one specimen and in the order of increasing strain.

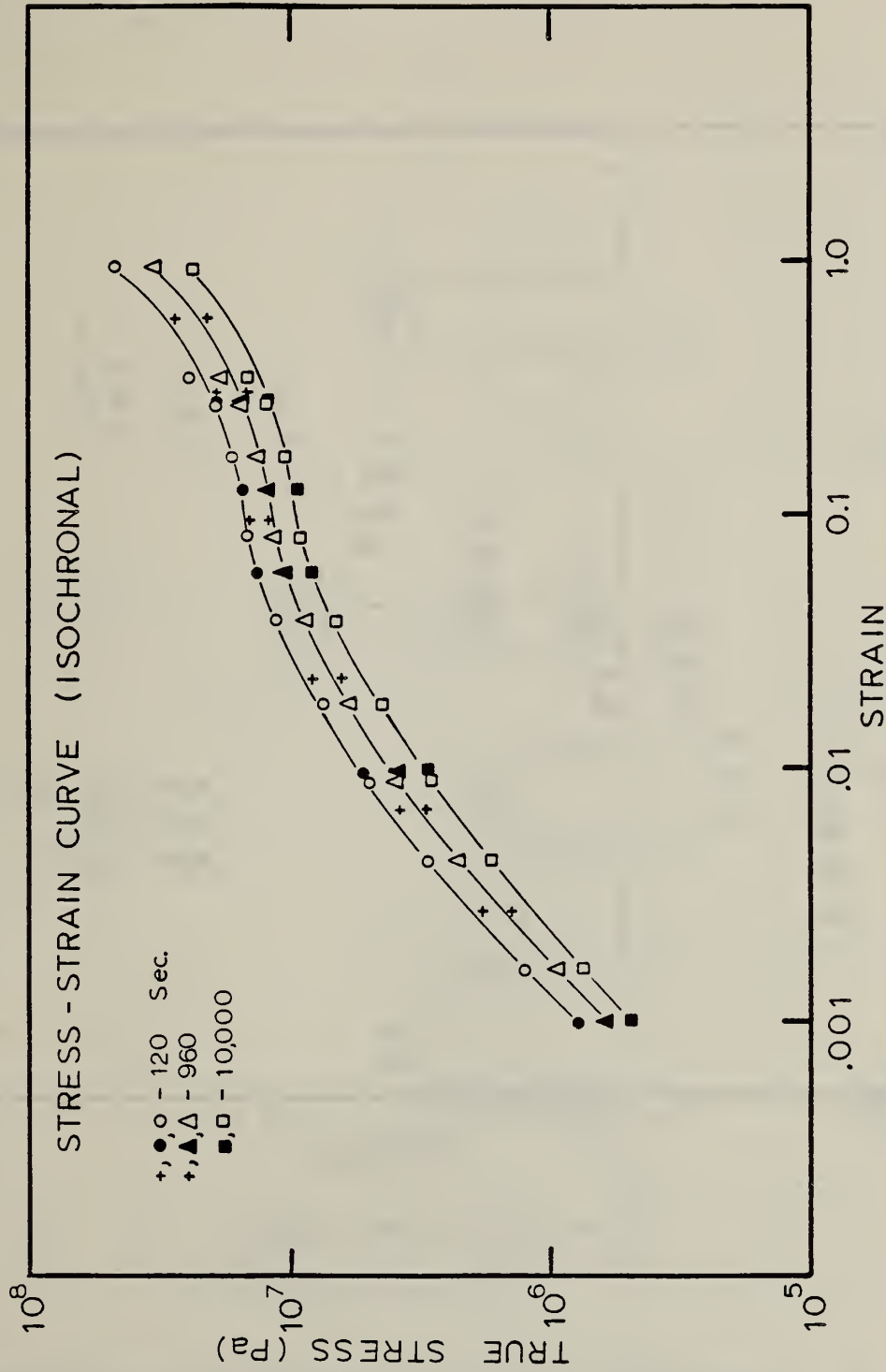


Fig. 14 Isochronal true stress versus strain for specimens of UHMWPE (UH-A) slowly cooled from 473K (200°C) - open symbols, and 438K (165°C) - filled symbols. Crosses are for samples of UHMWPE (UH-B) slowly cooled from 473K (200°C).

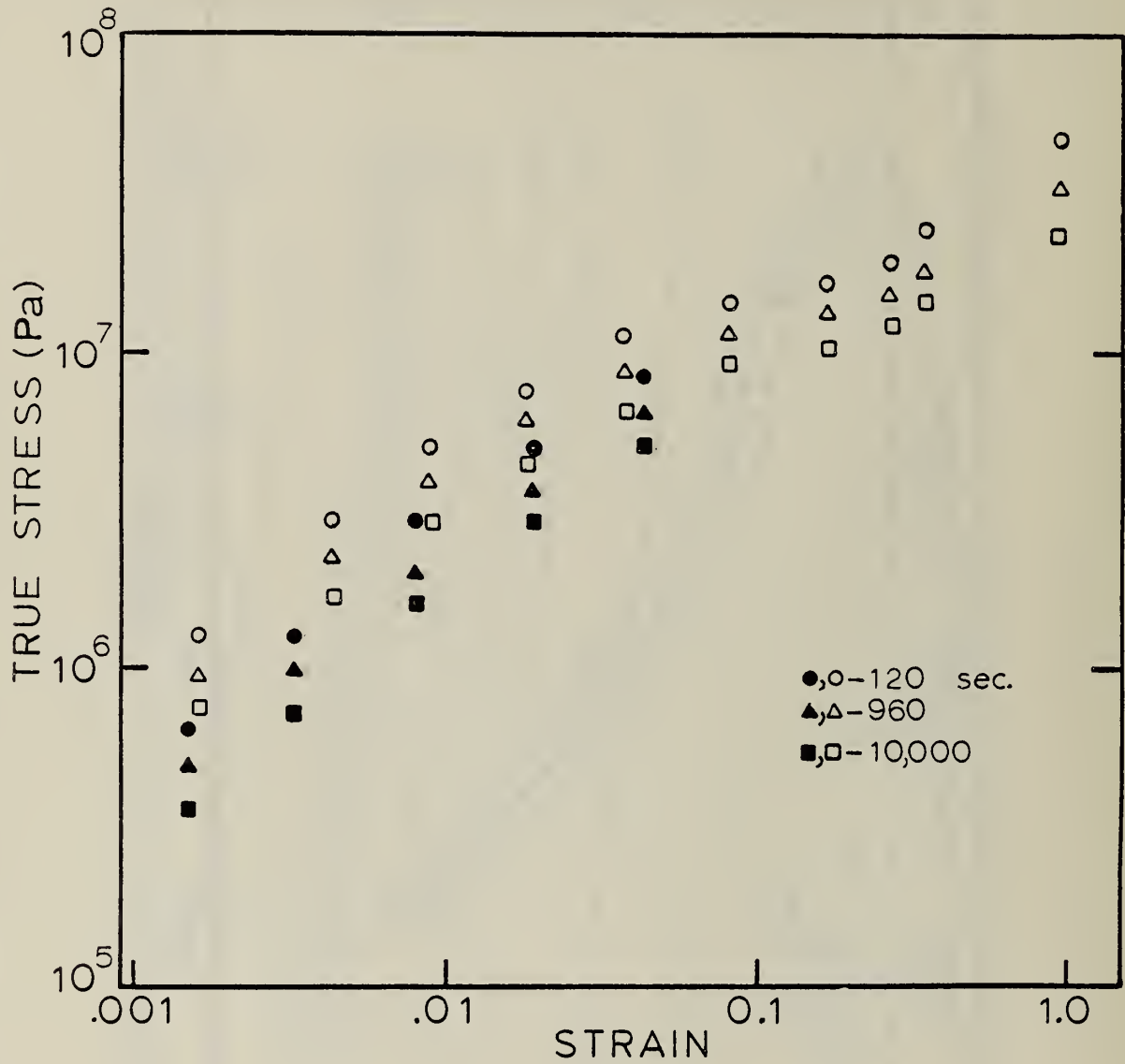


Fig. 15 Comparison of Isochronal Stress-Strain Data for UHMWPE (UH-A) specimens slowly cooled (open symbols) and quenched (filled symbols) from 473K (200°C).

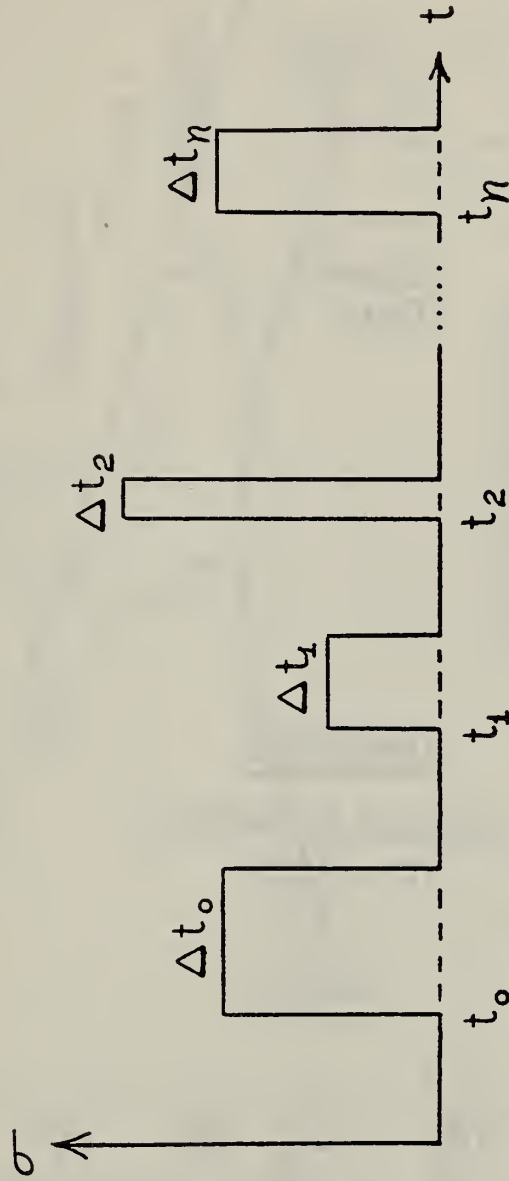


Fig. 16 Schematic representation of a possible loading history applied to a specimen of UHMWPE. See text for explanation of how the load during each time interval  $\Delta t_i$  would contribute to the damage accumulating in the material.

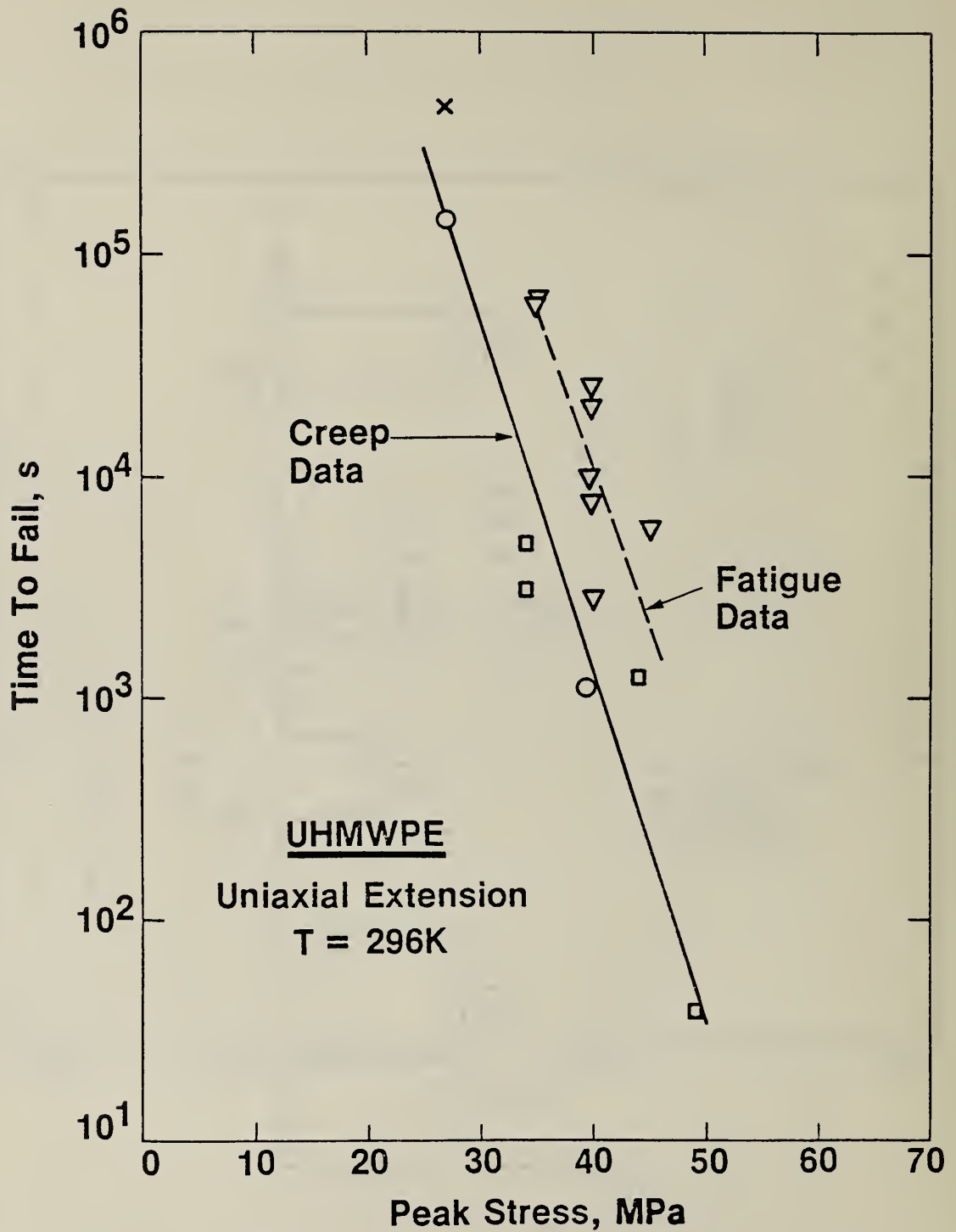


Fig. 17 Time to fail versus peak engineering stress for specimens of UHMWPE (UH-A) in creep (static fatigue) and zero-tension sinusoidal fatigue loading histories. The solid and dashed lines represent the linear regression curves for the data points shown. Samples were slowly cooled from the molding temperature, 0-438K(165°C); X-463K (190°C); □, ▽ - 473K (200°C).

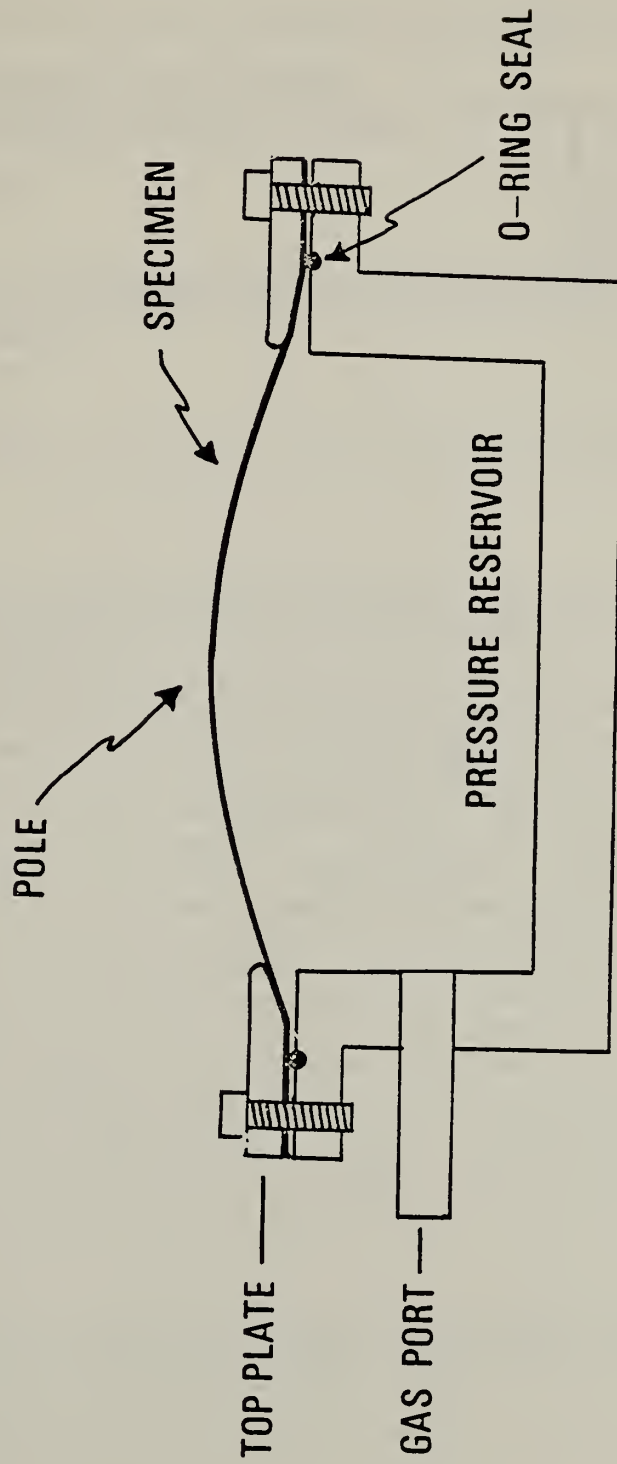
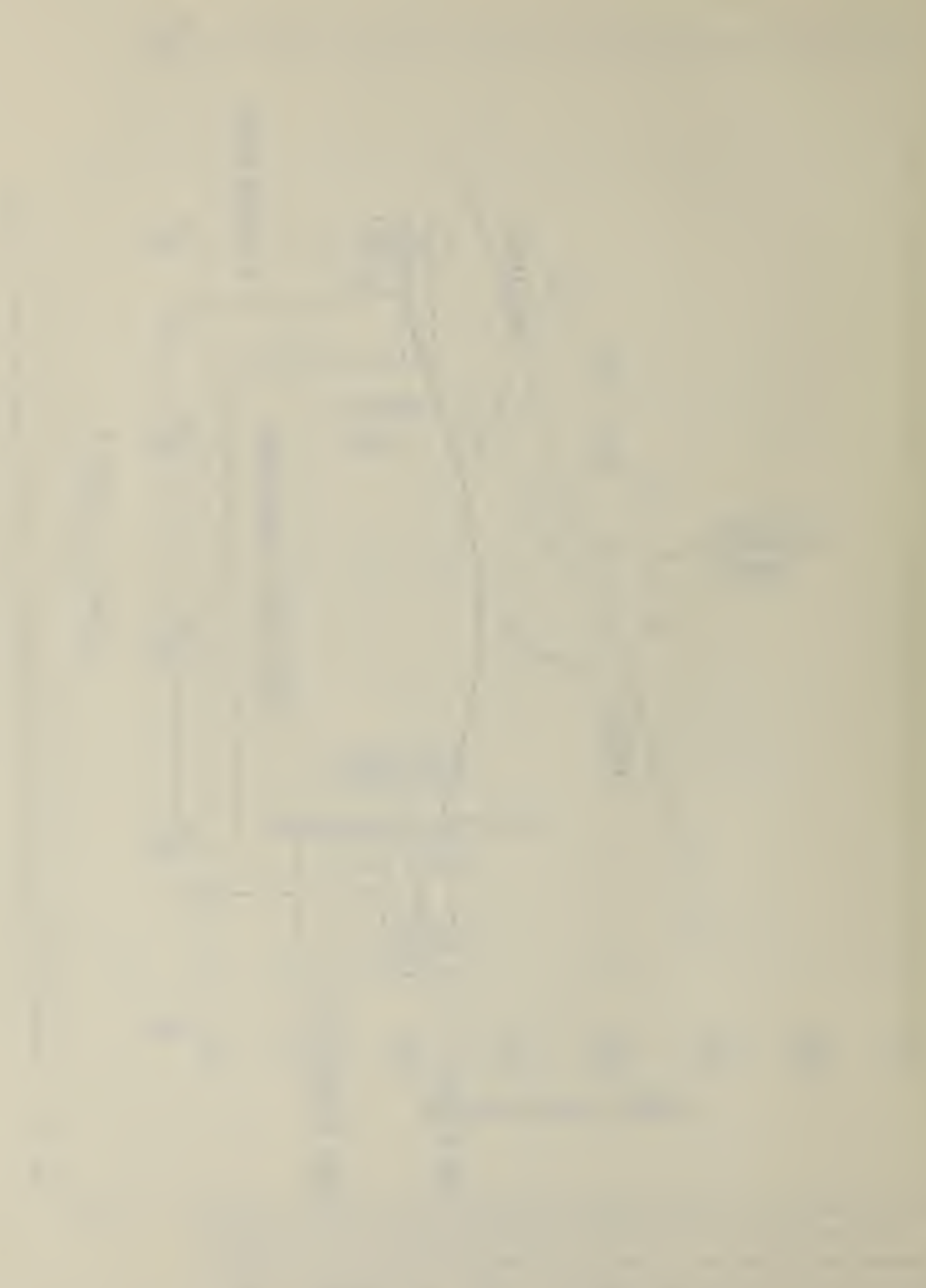


Fig. 18 Schematic diagram of inflation apparatus used for equal biaxial testing.



U.S. DEPT. OF COMM. <b>BIBLIOGRAPHIC DATA SHEET</b> (See instructions)	1. PUBLICATION OR REPORT NO. <b>NBSIR 81-2209</b>	2. Performing Organ. Report No.	3. Publication Date <b>December 1980</b>
4. TITLE AND SUBTITLE <b>Relationship Between Morphology and Mechanical Properties of Ultra High Molecular Weight Polyethylene</b>			
5. AUTHOR(S) <b>G.B. McKenna, F. A. Khoury and J.M. Crissman</b>			
6. PERFORMING ORGANIZATION (If joint or other than NBS, see instructions)  <b>NATIONAL BUREAU OF STANDARDS DEPARTMENT OF COMMERCE WASHINGTON, D.C. 20234</b>		7. Contract/Grant No.	8. Type of Report & Period Covered <b>Annual Report Dec. 9, 1979 - Sept. 30, 1980</b>
9. SPONSORING ORGANIZATION NAME AND COMPLETE ADDRESS (Street, City, State, ZIP) <b>Food and Drug Administration Bureau of Medical Devices 3257 Georgia Avenue Silver Spring, Md, 20910</b>			
10. SUPPLEMENTARY NOTES  <input type="checkbox"/> Document describes a computer program; SF-185, FIPS Software Summary, is attached.			
11. ABSTRACT (A 200-word or less factual summary of most significant information. If document includes a significant bibliography or literature survey, mention it here) Aspects of the morphology of the constituent particles of the raw ultra high molecular weight polyethylene (UHMWPE) used in this study have been examined using scanning electron microscopy. In addition differential scanning calorimetry has been used to determine the melting point (~413K) and the crystallinity (78%) of the raw polymer. Protocols have been established for the preparation of compression molded sheets of UHMWPE having crystallinities of 50% and 60%. A memory of the particulate nature of the raw polymer is retained in the sheets. The following aspects of the mechanical behavior of the molded sheets have been examined: Stress-strain behavior at constant rate of clamp separation, creep and single step stress relaxation in uniaxial extension, and failure under both static and sinusoidal loading conditions. The relaxation modulus of the lower density material (quenched) was found to be smaller by a factor or two than that of the higher density material (slow cooled). The short time creep of the quenched UHMWPE was significantly greater than that of the slow cooled polymer; however, the limiting creep strain prior to failure was nearly the same for both materials. Low cycle fatigue data obtained on the slow cooled UHMWPE suggests that it may be possible to characterize the failure behavior of this polymer using a cumulative damage rule. The lifetime of the UHMWPE under zero-tension sinusoidal loading is 6-7 times longer than the lifetime in static (creep) tests in agreement with the cumulative damage rule.			
12. KEY WORDS (Six to twelve entries; alphabetical order; capitalize only proper names; and separate key words by semicolons) <b>Ultra High Molecular Weight Polyethylene, UHMWPE, Morphology, Polymer, Mechanical Properties, Creep, Stress Relaxation, Fatigue, Failure.</b>			
13. AVAILABILITY <input checked="" type="checkbox"/> Unlimited <input type="checkbox"/> For Official Distribution. Do Not Release to NTIS <input type="checkbox"/> Order From Superintendent of Documents, U.S. Government Printing Office, Washington, D.C. 20402. <input checked="" type="checkbox"/> Order From National Technical Information Service (NTIS), Springfield, VA. 22161		14. NO. OF PRINTED PAGES <b>61</b>	15. Price <b>\$8.00</b>

